https://ntrs.nasa.gov/search.jsp?R=19670026752 2020-03-16T16:32:37+00:00Z

Faculty

Final **Report** | ***March** 1, 1964 to **June** 30, 1967*

STUDY OF GROWTH PARAMETERS FOR REFRACTORY CARBIDE SINGLE CRYSTALS

Prepared for:

OFFICE OF RESEARCH GRANTS AND CONTRACTS
CODE SC
NATIONAL AERONAUTICS AND SPACE ADMINISTRATION
WASHINGTON, D.C. 20546

CONTRACT NASr-49(19)

By: R. W. BARTLETT AND F. A. HALDEN

SRI Project FMU-4892

N67-36081
(ACCESSION NUMBER) (THRU)
10109 TS 22-25 1
(PAGES) (CODE)
CR-88354 END 17
(NASA CR OR TMX OR AD NUMBER) (CATEGORY)
FACILITY FORM 602

STANFORD RESEARCH INSTITUTE
MENLO PARK, CALIFORNIA

GPO PRICE $ _____
CFSTI PRICE(S) $ _____
Hard copy (HC) 3.00
Microfiche (MF) .65
ff 653 July 65

STANFORD RESEARCH INSTITUTE
MENLO PARK, CALIFORNIA

9 June 30, 7967 10 CV

4 Final Report 1 March 7, 7964 to June 30, 7967 6

3 STUDY OF GROWTH PARAMETERS FOR REFRACTORY CARBIDE SINGLE CRYSTALS 4

Prepared for:

OFFICE OF RESEARCH GRANTS AND CONTRACTS
CODE SC
NATIONAL AERONAUTICS AND SPACE ADMINISTRATION
WASHINGTON, D.C. 20546

CONTRACT NASr-49(19)

1
25

By: 6 R. W. BARTLETT AND F. A. HALDEN 9

SRI *Project* FMU-4892

Approved: A. E. GORUM, ASSOCIATE EXECUTIVE DIRECTOR
MATERIAL SCIENCES LABORATORIES

Copy No. 15

PRECEDING PAGE BLANK NOT FILMED.

FOREWORD

The research described in this report was performed at Stanford Research Institute under Contract NASr-49(19) with the Office of Research Grants and Contracts, National Aeronautics and Space Administration. Dr. H. B. Probst was the Project Monitor. The assistance of Mr. James J. Gangler is gratefully acknowledged.

This report covers work conducted between 1 March 1964 and 30 June 1967. The principal investigators were F. A. Halden and R. W. Bartlett. The authors wish to acknowledge the assistance of J. W. Fowler, melt growth; W. E. Nelson, solution growth; J. B. Saunders, X-ray diffraction; H. J. Eding, vaporization and stoichiometry calculations; and C. W. Smith, sound velocity measurements.

PRECEDING PAGE BLANK NOT FILMED.

PRECEDING PAGE BLANK NOT FILMED.

ABSTRACT

The feasibility of growing single crystals of the most refractory metal carbides from their melts and from liquid metal solutions was investigated. Boules produced by an a-c arc-heated Verneuil technique yielded cut single crystals of tantalum monocarbide and hafnium monocarbide. Crystals of tantalum monocarbide up to 1 inch long were obtained. Spontaneous nucleation of new grains during crystal growth usually prevented the harvesting of crystals longer than 0.4 inch. Mixed tantalum carbide/hafnium carbide solid-solution crystals large enough for physical property measurements were not obtained because of excessive nucleation during growth. The carbon content of tantalum monocarbide crystals was lowered to 43-46 atomic percent by vaporization of carbon during crystal growth. Further carbon depletion was prevented by using a hydrogen/argon gas mixture. The elastic constants of $TaC_{0.9}$ crystals were determined by an ultrasonic method. Verneuil melt growth using induction plasma heating was unsuccessful. Liquid metal solution growth did not yield crystals larger than 0.2 mm.

PRECEDING PAGE BLANK NOT FILMED

CONTENTS

CONTENTS (Concluded)

ILLUSTRATIONS

ILLUSTRATIONS (Concluded)

TABLES

I INTRODUCTION

Interest in refractory carbide compounds has increased considerably in recent years as a result of the increasing number of aerospace applications requiring materials that are stable above 2500°C. Such applications are in reentry systems, rocket nozzles, electrical propulsion devices, and other high temperature structures. Unfortunately, insufficient basic information is available to assist in the evaluation of the most refractory of these compounds, tantalum carbide, hafnium carbide, and their mixed solid solutions. The purity of these compounds has generally been poor; fabrication of dense, reliable shapes is difficult; and single crystals have not been available. To obtain much of the data on physical characteristics of these materials, single crystal specimens are required. The National Aeronautics and Space Administration has therefore engaged Stanford Research Institute to investigate the feasibility of selected crystal growth methods for preparing these single crystals.

A. Objectives

The program has been restricted to tantalum carbide, hafnium carbide, and mixed solid solutions of these two carbides. The objectives of the program were:

1. To determine the feasibility of and procedures for applying recently developed liquid-metal solution crystal growth techniques and new heating methods for Verneuil crystal growth to preparation of the refractory carbide single crystals.
2. To grow, using the most promising technique, single crystals of refractory carbides and to characterize these crystals.
3. To establish the feasibility of controlling crystal stoichiometry and structure by modifications in the crystal growth environment.

B. Technical Background

1. Refractory Carbides

The most recent phase diagrams[2] for the tantalum-carbon and hafnium-carbon systems are shown in Figs. 1 and 2, respectively. Two compounds are found in the tantalum carbon system with nominal compositions Ta_2C and TaC. Only one compound, HfC, exists in the hafnium-carbon system, This program is concerned with crystal growth of the monocarbides, which have the highest melting points of all congruently melting substances. These compounds are completely miscible solids, with the NaCl structure. Because of the very small size of the carbon atoms, they occupy the interstices of a face-centered cubic array of the larger metal atoms. Consequently, carbon vacancies are easily tolerated, permitting the wide homogeneity range shown in the phase diagrams.

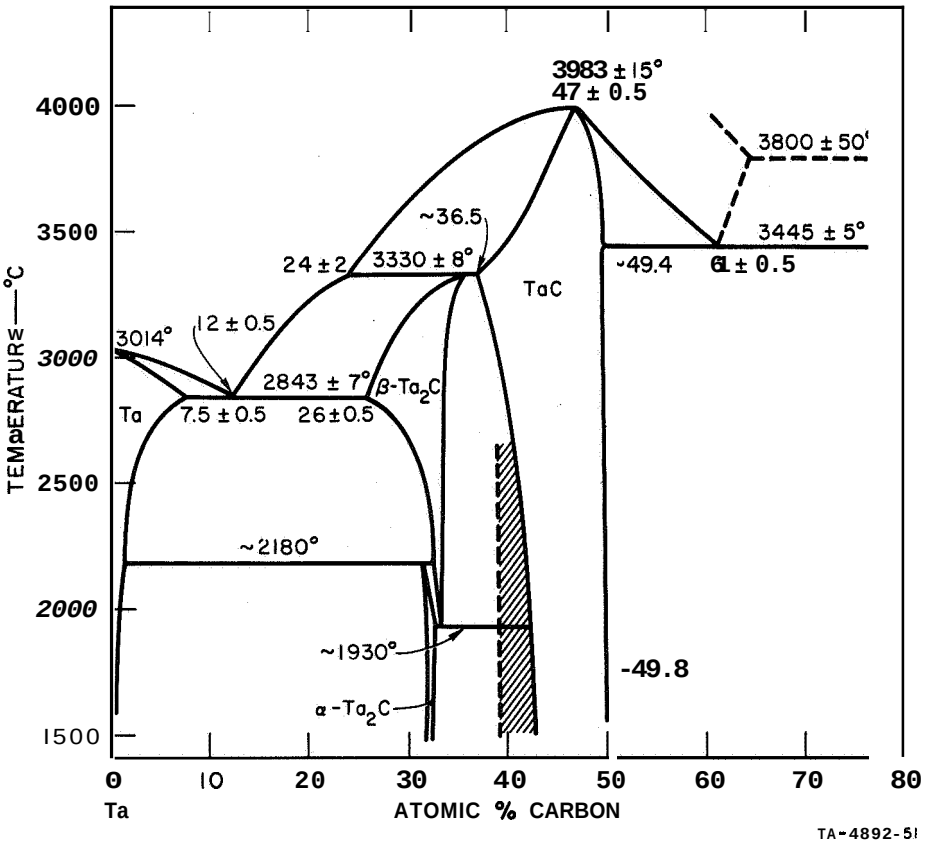

FIG. 1 PHASE DIAGRAM OF THE SYSTEM TANTALUM–CARBON (from Rudy and Harmon')

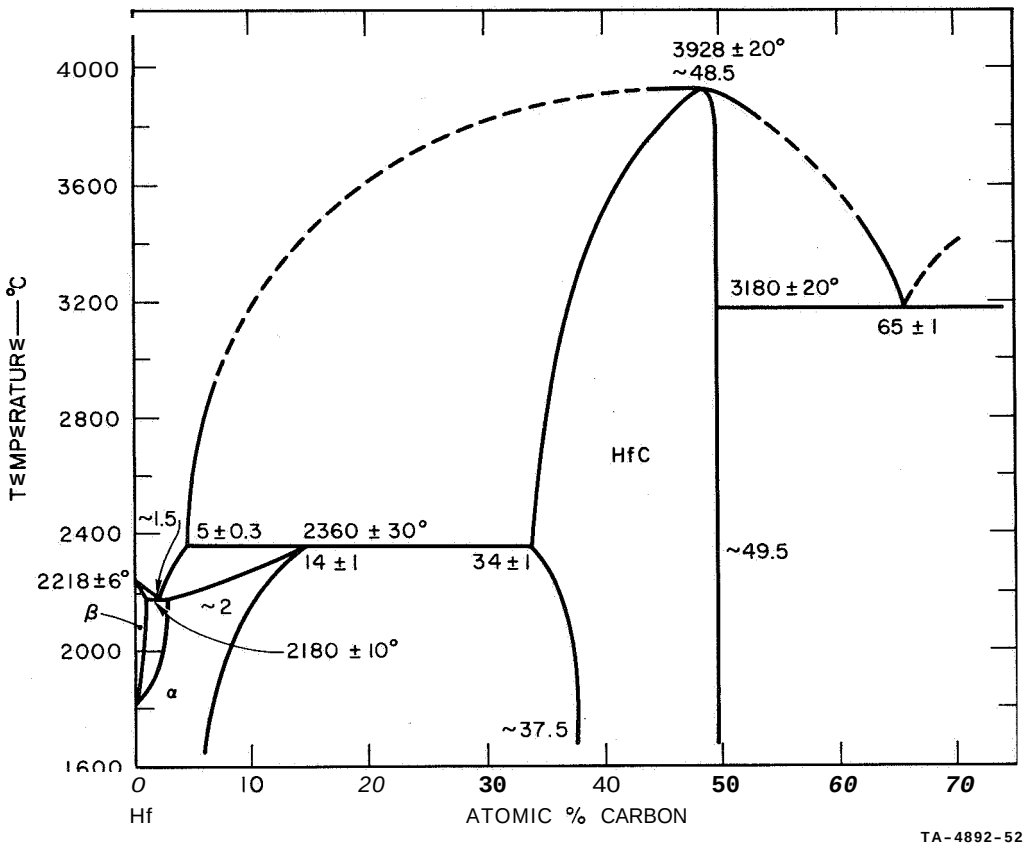

FIG. 2 PHASE DIAGRAM OF THE SYSTEM HAFNIUM–CARBON (from Rudy[2])

2. Crystal Growing Methods

Although there are a number of techniques for growing crystals, most of the major methods can be grouped into three general classes: (a) growth from the melt, (b) growth from solution, and (c) growth from a vapor phase. Each of these methods has certain advantages and limitations for growth of the refractory carbides.

a. Melt Growth

Melt growth offers the greatest potential for producing large single crystals of refractory carbides at reasonable growth rates. Ideally, in all modifications of this general technique, the melt is maintained slightly above the melting point, while the crystallizing solid is held just below the melting temperature. Once growth is

completed, the crystal is cooled to room temperature under conditions minimizing thermal gradients through the crystal in order to minimize residual stresses. Attainment of the high temperatures required to melt these carbides is the major obstacle to the use of melt growth. Other difficulties associated with the high melting temperatures include the following: (1) high defect concentrations invariably occur; (2) vaporization rates of the components of each carbide are high, and selective depletion of the carbon occurs in tantalum carbide; (3) shifts in stoichiometry can be quite large within the monocarbide phase; and (4) stresses induced thermally during crystal growth or during cooling may be vary large.

In the present study, two heating methods were investigated: an induction-coupled plasma torch and an electric arc discharge. The induction-coupled plasma torch provides a large diameter, low velocity plasma in the vicinity of a crystal boule. By suitable manipulation, this plasma can simulate the geometry of the combustion flame employed in the normal Verneuil process. Since the induction plasma does not require electrodes or other apparatus components in contact with the plasma, chemically reactive gases such as methane or halogens can be used without extensive corrosion of the apparatus or contamination of the growing crystals by the apparatus.

An arc discharge is capable of generating very high temperatures. Since the carbides are electrically conducting, arc melting by direct discharge of the arc to a growing crystal boule is feasible.

Other melting procedures, including electron beam heating and arc image heating, were considered and found to be unsuitable for attaining the required temperatures in the atmospheres needed to control vaporization. Consequently, experimental work on melt growth was restricted to the induction plasma and arc heating methods.

b. Solution Growth

Since solution growth of refractory carbides in metal menstruums can be accomplished at much lower temperatures than melt growth,

many of the expected disadvantages of melt growth are not likely to be encountered in solution growth experiments. However, there are other potential obstacles to growth of large crystals by the solution method: (1) inadequate solubility of carbon, tantalum, or hafnium in potential solvents; (2) excessive spontaneous nucleation of crystals; (3) chemical reactions involving the crucible or seed holder materials; and (4) contamination of the crystals by the solvent. Liquid metal solution crystal growth techniques were investigated in the present program.

c. Vapor Growth

Vapor growth of carbides by the Van Arkel and similar processes has been used for many years to prepare high purity carbides. In this technique, a halide of the metal is normally reacted with hydrogen and a hydrocarbon, or a pyrolytic process is employed, to deposit the carbide on a hot surface. This method suffers from low growth rates and difficulties in preventing random crystal nucleation. Consequently, it does not appear sufficiently promising for producing large single crystals of the refractory carbides and was not investigated in the present program.

II SUMMARY

Boules of $TaC_{\sim 0.9}$ and HfC were grown from the melt using ac arc heating (Verneuil method). The hafnium carbide boules were fully carburized; the tantalum carbide boules had a carbon content of 43 to 46 at.% ($TaC_{\sim 0.9}$) but were free of the Ta_2C phase. Spontaneous nucleation of new grains during crystal growth was the major problem hindering the harvesting of large single crystals. Although most boules contained large grains, only a few of the tantalum carbide boules were entirely free of grain boundaries. Nevertheless, cut single crystal bars of tantalum carbide up to one inch in length were produced. Mixed solid solution boules were grown from 20% HfC/80% TaC and 40% HfC/60% TaC powders. Grain boundary density was somewhat higher in mixed solid solution boules in single carbides. The principal reason for excessive nucleation in these compositions was probably the poor control obtained over the starting carbide powders.

Solution growth yielded carbide crystals from a variety of menstruums, but crystal size did not exceed 0.2 mm. Nucleation of fine carbide crystals and continuous dispersion of these crystals throughout the metal solution, caused by free convective mixing of the solution, prevented growth of larger crystals.

Induction plasma heating was not capable of melting stoichiometric tantalum carbide or hafnium carbide.

III MELT GROWTH BY ARC HEATING

Considerable effort was directed toward developing a direct arc melting system suitable for Verneuil crystal growth of tantalum carbide and hafnium carbide. This effort consisted of (1) a preliminary test phase to determine the feasibility of arc melting; (2) design and operation of a preliminary direct arc crystal grower; and (3) design and operation of a larger arc crystal grower incorporating several design improvements dictated by the operating experience with its predecessor.

A. Feasibility Studies with Tantalum Carbide and Hafnium Carbide

The feasibility of using arc melting for Verneuil growth of the refractory carbides was explored by (1) a literature review, and (2) preliminary arc melting tests. Considerable attention was paid to vaporization of the crystal components and control of crystal stoichiometry. The literature findings are summarized in Appendix A. The results indicated that control of stoichiometry during melting would not be too difficult for hafnium carbide. Tantalum carbide was expected to lose carbon during melting, but it appeared likely that the composition could be maintained within the monocarbide homogeneity range by using carburizing gas environments.

Preliminary arc melting tests were made on small polycrystalline tantalum carbide and hafnium carbide bodies to determine the feasibility of the arc heating method and to measure changes in stoichiometry resulting from vaporization occurring during melting. The furnace used for these tests provided for introducing two horizontal 1/4-inch carbon electrbdes and one vertical crystal support pedestal. No provision for rotation of the electrodes or seeds was made. Both dc and ac arc melting tests were made using ballast resistors or saturable core reactors to match the arc load characteristics with available power supplies.

When the pedestal was insulated to prevent arc discharge through the carbide, melting of the refractory carbides inserted between the electrodes could not be achieved. When the crystal support pedestal was grounded, rather than insulated, and used as part of the arc circuit, both tantalum carbide and hafnium carbide melted at relatively low power levels. To increase the symmetry of the molten cap, two electrodes were discharged to the carbide sample and, later, in the final crystal growing furnace, three horizontal electrodes were used.

Several tests were made to examine changes in stoichiometry resulting from melting hafnium carbide and tantalum carbide in various gaseous environments. For these tests, hafnium carbide was hot-pressed at 3500 psi and 2300°C, as recommended by Sanders and Grisaffe,[3] to form circular discs 1 inch in diameter and 0.1 inch thick having a density of approximately 85% of theoretical. These discs were cut to form rods 0.1 inch square and 1/2 to 1 inch in length. Plasma-sprayed tantalum carbide in the form of rods was also used in some of the tests. Density of these samples was approximately 75% of theoretical. These rods were melted in the arc furnace in the presence of argon, hydrogen, acetylene, and mixtures of these gases. The melts were held at temperature for periods of 1 to 5 minutes. Samples were then quenched and sectioned through the previously melted zone. The top portion (melt cap) was ground for X-ray evaluation of the carbide lattice parameter, and the cut face of the lower portion was polished for metallographic examination.

Figure 3 shows a composite curve[4-6] for lattice constant as a function of carbon content in the lattice. Using the data from Fig. 3, the carbon content (stoichiometry) of melted tantalum carbide samples was determined. The literature data on lattice parameter variation with carbon content for hafnium carbide are not in good agreement. The most recent data of Rudy[2] are shown in Fig. 4.

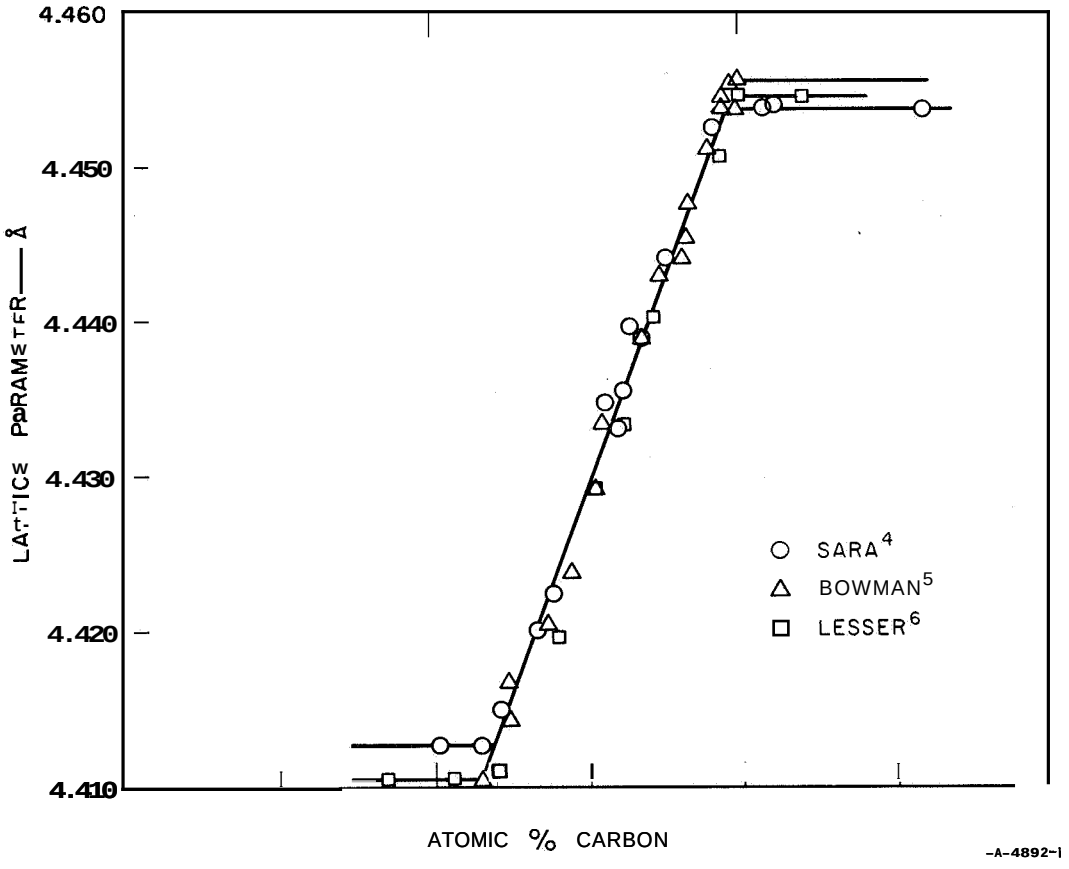

FIG. 3 VARIATION OF LATTICE PARAMETER WITH CARBON CONCENTRATION IN TaC_{1-x}

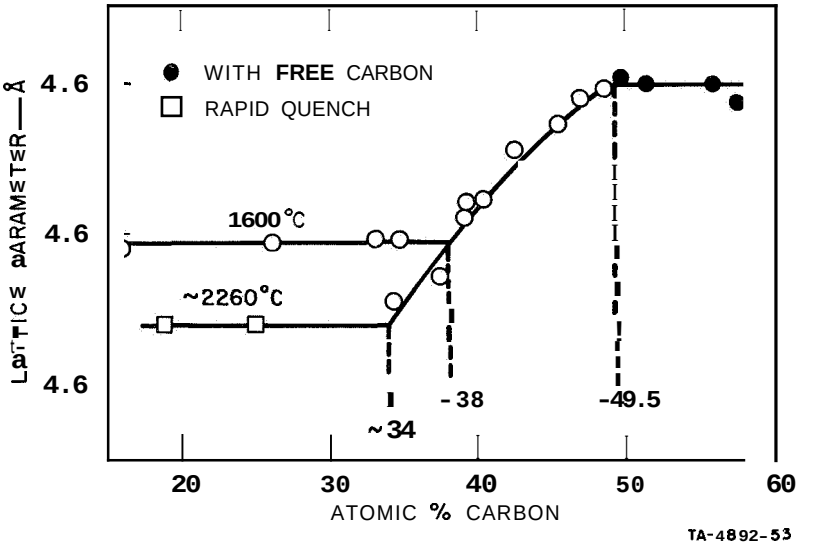

FIG. 4 VARIATION OF LATTICE PARAMETER WITH CARBON CONCENTRATION IN HfC_{1-x} (from Rudy[2])

Some of the data for both arc-melted tantalum carbide and hafnium carbide are shown in Table I. Fortunately, with the exception of one sample melted in argon, the hafnium carbide samples showed some increase in lattice parameter and carbon content after melting. Further tests in the crystal growth furnace showed that the stoichiometry shifts of hafnium carbide in 10% argon were negligible at 1 atm pressure if the hot carbon electrodes were closely spaced. This is in agreement with Deadmore's findings[7,8] that the vaporization rates of hafnium and carbon from hafnium carbide are approximately equal. Consequently, there is no shift in stoichiometry even though the rate of evaporation of hafnium carbide at high temperatures is quite rapid.

In tantalum carbide, the evaporation rate of tantalum is much lower than the evaporation rate of carbon and, consequently, carbon becomes depleted from the melt. This phenomenon lowers the melting point (solidus) and if carried to completion will result in precipitation of the hexagonal close-packed Ta_2C phase after solidification

Table I

LATTICE PARAMETERS OF ARC-MELTED MONOCARBIDES

Carbide	Melt Treatment		Lattice Parameter (Å)	Carbon (At.%)	Number of Phases
	Time (min)	Gas Environment			
TaC	0	Starting powder	4.456 ± 0.001	49.5	1
	5	95 Ar/5 H_2	4.451 ± 0.002	49.0	1
	5	90 Ar/10 H_2	4.437 ± 0.002	46.5	1
	5	80 Ar/20 H_2	4.434 ± 0.002	46.0	1
	5	60 Ar/40 H_2	4.424 ± 0.002	44.0	1
	5	100 H_2	4.449 ± 0.002	48.0	1
	1	100 H_2	4.436 ± 0.002	46.0	1
	5	85Ar/10H_2/5C_2H_2	4.428 ± 0.005	44.5	1
	5	100 Ar	4.418 ± 0.002	42.0	2 (Ta_2C)
	1	95 Ar/5 C_2H_2	4.414 ± 0.002	42.0	2 (Ta_2C)
HfC	0	Starting powder	4.631 ± 0.001	43.0	1
	0	Hot pressed	4.632 ± 0.001	43.5	1
	5	100 Ar	4.618 ± 0.001	38.0	1
	1	70 Ar/30 H_2	4.633 ± 0.001	44.0	1
	5	95 Ar/5 C_2H_2	4.640 ± 0.001	49.0	1
	1	100 H_2	4.642 ± 0.001	49.5	1

and further cooling. The precipitation of Ta_2C occurs on low index planes of the TaC lattice and provides a Widmanstätten structure that is visible after polishing and etching the sample.' Appearance of the Widmanstätten structure is a rather sensitive indicator of precipitation of Ta_2C. When only small amounts of Ta_2C were produced, the precipitates were usually found near the grain boundaries, as shown in Fig. 5(a). When larger amounts of Ta_2C were present, the Widmanstätten structure was observed throughout the monocarbide field, as shown in Fig. 5(b).

Brauer's zeta TaC_{1-x} phase,[6] a pseudomorph that has been reported to form epitaxially on substoichiometric TaC, was not identified in any of the many samples examined by X-ray diffraction. This result is explained by the recent observation[1] that zeta TaC_{1-x} only forms when cooling from temperatures below 2500°C, in the region of the shaded area in the phase diagram of Fig. 1.

The carbon contents of the starting materials listed in Table I are not unexpectedly low. As the phase diagrams show, the carbon lattice positions in tantalum carbide and hafnium carbide (interstices in a FCC tantalum and FCC hafnium lattice) are never completely filled. The carbon contents at the maximum melting points are 47 at.% for tantalum carbide and 48.5 at.% for hafnium carbide.

Methods were sought to retard the loss of carbon during the melting of tantalum carbide. Additions of hydrocarbons which could contribute carbon to the atmosphere and partially compensate for the loss of vaporized carbon were employed. As will be shown in Appendix A, acetylene is, from a thermodynamic viewpoint, the most favored common gas for this purpose. However, hydrogen additions to argon were found to be more effective than addition of hydrocarbon gases. It appears that hdyrogen reacts with the hot carbon electrodes to transfer carbon to the molten boule. Small additions of hydrogen, 5 to 10%, are sufficient to maintain the carbon content at 45 at.% and well within the composition field of the TaC phase. These tests were performed at a

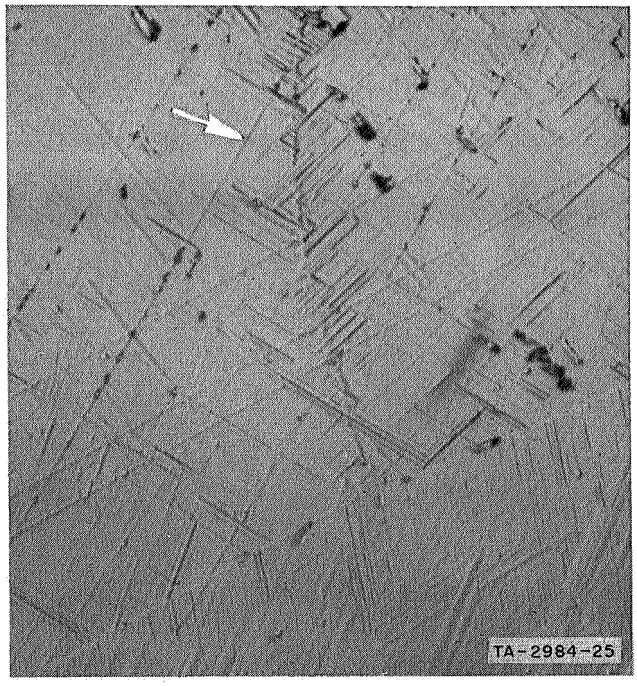

(a)

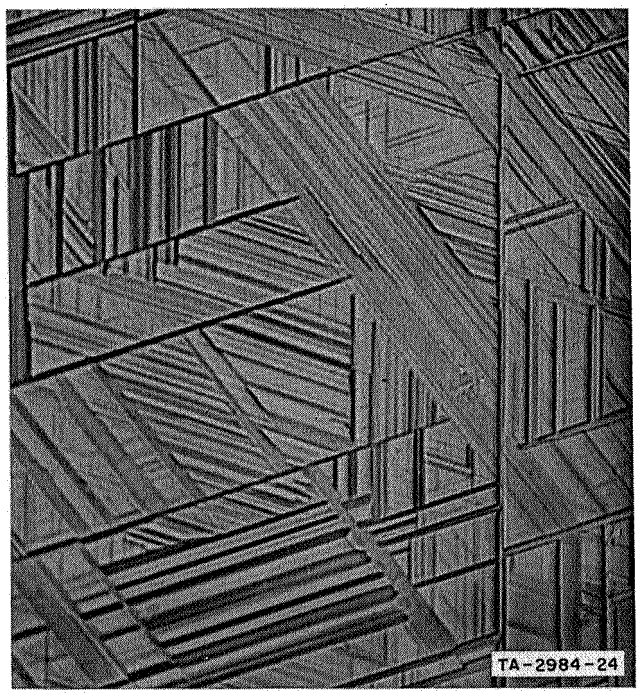

(b)

FIG. 5 (a) LIGHT Ta_2C PRECIPITATION IN THE INTERIOR OF THE BOULE WITH PREFERRED PRECIPITATION ALONG SUBGRAIN BOUNDARIES (arrow); (b) HEAVY Ta_2C WIDMANSTÄTTEN PRECIPITATION NEAR SURFACE OF BOULE; ETCHED, 1600X

total pressure of 1 atm. In subsequent tests, it was determined that if the total pressure drops below approximately 200 mm Hg, carbon depletion is extensive and Ta_2C results regardless of the environmental gas used.

B. Vaporization and Stoichiometry of Hafnium Carbide/Tantalum Carbide Mixtures during Melt Growth

Experiments with mixed solid solution carbides were not attempted until the complete crystal growing apparatus was operating. Boules grown from mixed solid solution carbide powders showed some loss of carbon and depletion of hafnium during melt growth. However, results were in excellent agreement with the behavior based on extrapolating Deadmore's data[8] for mixed solid solution carbides taken at 2600°C and lower temperatures.

X-ray diffraction analyses and X-ray fluorescent analyses, with a LiF monochrometer, were used to determine changes in metal compositions and estimate carbon losses for several boules. Standard curves were made, plotting relative hafnium and tantalum X-ray fluorescent intensity (peak height/sum of peak heights for both hafnium and tantalum) versus the known metal composition of several carbides. The tantalum L_α and hafnium L_α fluorescent peaks were used. These curves, shown in Fig. 6, were made with the following starting powders: tantalum carbide, hafnium carbide, 40% hafnium carbide/60% tantalum carbide, and 20% hafnium carbide/80% tantalum carbide.

Lattice parameters were determined for these same materials using X-ray diffraction. These data, shown as closed circles in Fig. 7, conform reasonably well with a linear relationship between lattice parameter and composition for our starting powders of solid solution carbide mixtures. There was considerable line broadening of the 40% hafnium carbide/60% tantalum carbide, indicating incomplete homogenization of this starting material. Similar lattice parameter data by Deadmore' are shown as open circles in Fig. 7.

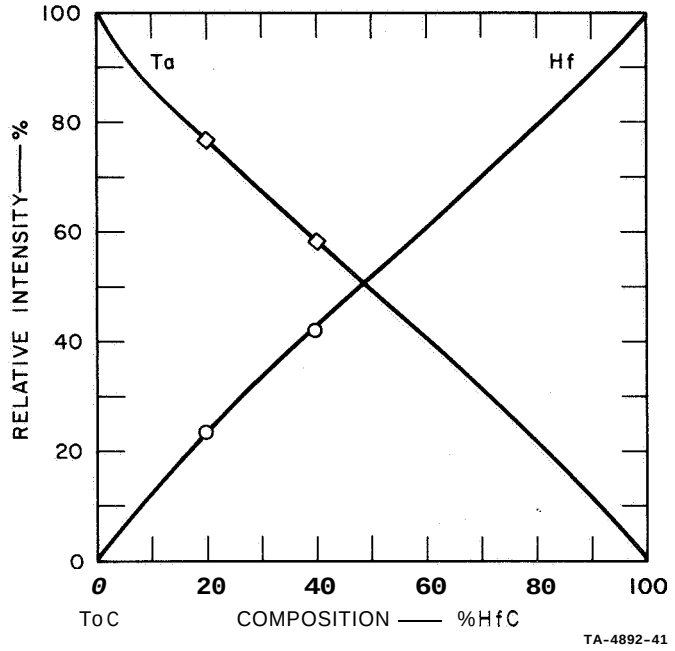

FIG. 6 RELATIVE X-RAY INTENSITY vs COMPOSITION FOR FLUORESCENT ANALYSIS OF MIXED CARBIDE SOLID SOLUTIONS

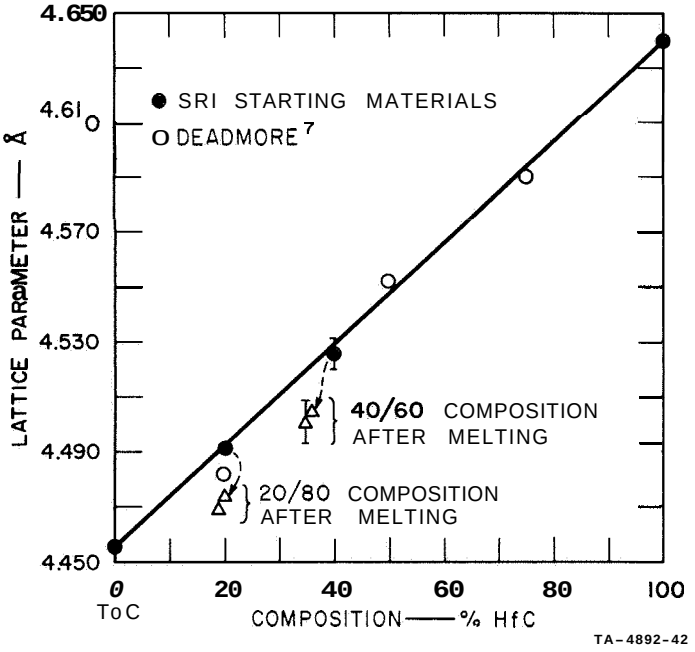

FIG.7 LATTICE PARAMETER vs METAL RATIO FOR FULLY CARBURIZED MIXED CARBIDE SOLID SOLUTIONS

Fluorescent analyses of crushed boules are given in Table 11. These analyses used the standard curves of Fig. 6. Although there was some loss of carbon in these boules, this is not expected to affect the metal analyses because of the low total carbon content and low X-ray absorption coefficient of carbon.

Table II

X-RAY ANALYSES OF MIXED CARBIDE BOULES

Carbide Powder Composition	Run No.	Atmosphere	Boule Metal Composition	
			%Hf	%Ta
40% HfC 60% TaC	9-30-2(66)	Argon, 1 atm	36	64
40% HfC 60% TaC	10-5-1(66)	10% H_2-Ar, 1 atm	35	65
20% HfC 80% TaC	10-6-1(66)	Argon, 1 atm	19	81
20% HfC 80% TaC	10-7-1(66)	5% H_2-Ar, 1 atm	20	80

It can be seen from Table II that the hafnium content in the 40/60 carbide decreased from 40% to about 35% of the total metal content of the boules, while the hafnium content of the 20/80 carbide did not change significantly. These data agree with the relative hafnium and carbon vaporization rates determined by Deadmore[8] for mixed hafnium carbide/tantalum carbide solid solutions. Deadmore's data are reproduced in Fig. 8. The hafnium and tantalum vaporization rates are almost equal at the 20% hafnium carbide/80% tantalum carbide composition, and therefore the metal ratio will not change while the compound is held at vaporizing temperatures. At the 40% hafnium carbide/60% tantalum carbide composition, the hafnium vaporization rate is significantly higher than that of tantalum, causing a reduction in the hafnium/tantalum ratio of the residual carbide upon heating to vaporizing temperatures.

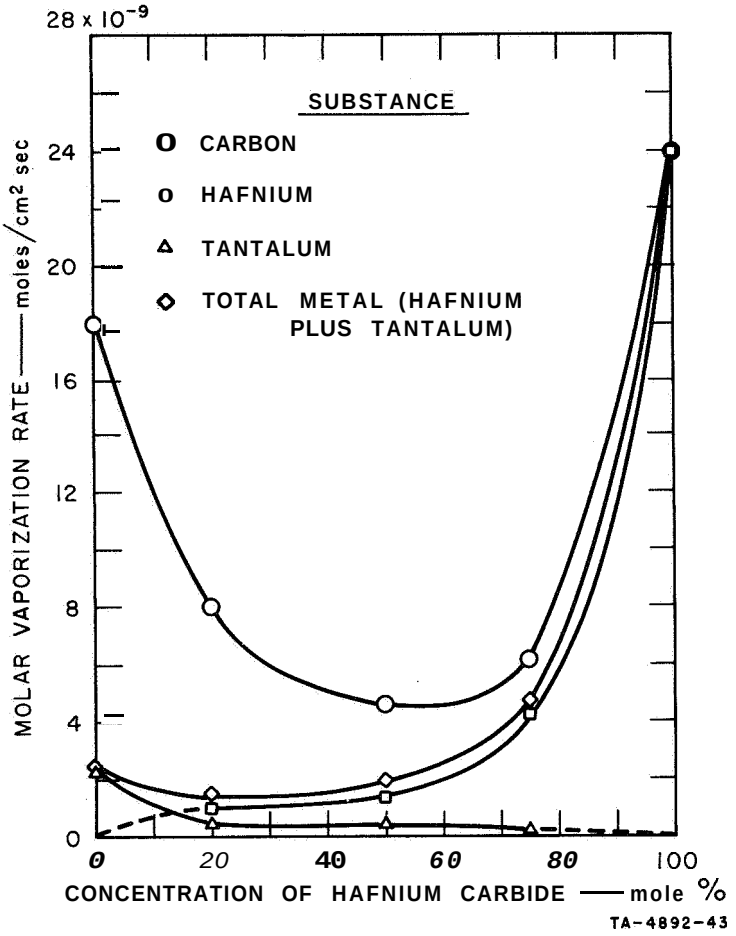

FIG. 8 MOLAR VAPORIZATION RATES OF CARBON, HAFNIUM, TANTALUM, AND TOTAL METAL (hafnium plus tantalum) FOR TANTALUM CARBIDE–HAFNIUM CARBIDE AT 2600°C IN VACUUM. Calculated from 20-hour sublimate compositions and instantaneous vaporization rate. (after Deadmore[8])

For all compositions of these mixed carbides other than 100% hafnium carbide, the carbon vaporization rate exceeds the total metal vaporization rate and there is a net loss of carbon in the residue as a result of heating or boule growth. The carbon loss is accompanied by a reduction in lattice parameter (see Fig. 7). The change in lattice parameter with carbon content is unknown for the mixed carbide compounds, but can be inferred from a weighted average of similar data for hafnium carbide[2]

and tantalum carbide.[4-6] This comparison indicates a carbon content of 45–47 at.% for the 20/80 carbide boules and 44–46 at.% for the 40/60 carbide boules.

C. Apparatus Design

Figures 9 and 10 show the major design features of the final (Model 2) arc Verneuil furnace. It consists of an 8-inch-diameter water-cooled vacuum chamber into which three horizontal electrodes and a boule holder are inserted. The boule holder enters through the bottom flange and acts as a common ground electrode, and the smaller horizontal electrodes discharge to the boule. The three horizontal electrodes are oriented 120° from each other and have a common projected intersection at the axis of the boule holder. Loci of all four intersecting axis are maintained within a 0.25 mm diameter region during rotation of the electrodes and boule.

The boule holder is a centerless-ground stainless steel rod, 1 inch in diameter, supporting a high purity (National Carbon Grade AUC) graphite pedestal. The boule holder is rotated and lowered by means of two variable speed motors mounted on a carriage beneath the furnace. Four segmented copper-graphite brushes mounted below the furnace provide electrical contact to the boule holder and help to remove heat. Additional heat is removed through two copper-graphite sleeve bearings, mounted above and below the brushes. A double quad ring seal (Viton) permits evacuation of the furnace chamber. Since most of the feed powder collects at the bottom of the furnace chamber, an insulating boron nitride cover-plate surrounds the boule holder at the bottom of the furnace and prevents carbide particles from falling into the seal and bearing housing. Carbide particles which collect in the bottom of the furnace are periodically removed with a vacuum probe.

The horizontal electrodes are similar to the vertical boule holder. Sizes are scaled down because of the lower power requirements for each of the three horizontal electrodes. The horizontal electrodes are rotated at a fixed speed, 1 rpm. The stand-off distance or gap separating

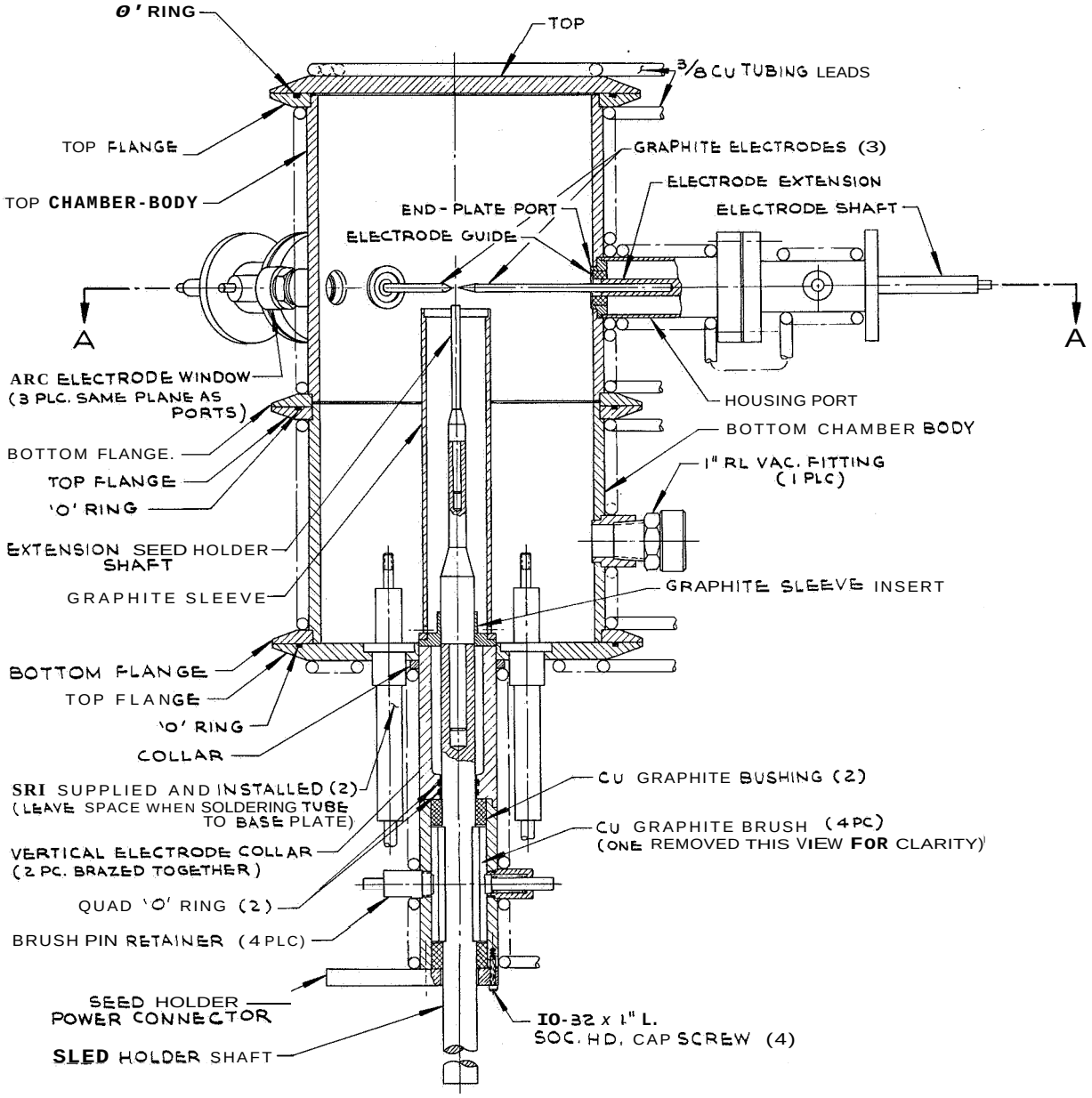

FIG. 9 FRONT VIEW OF ARC–VERNEUIL FURNACE MOD 2 ASSEMBLY

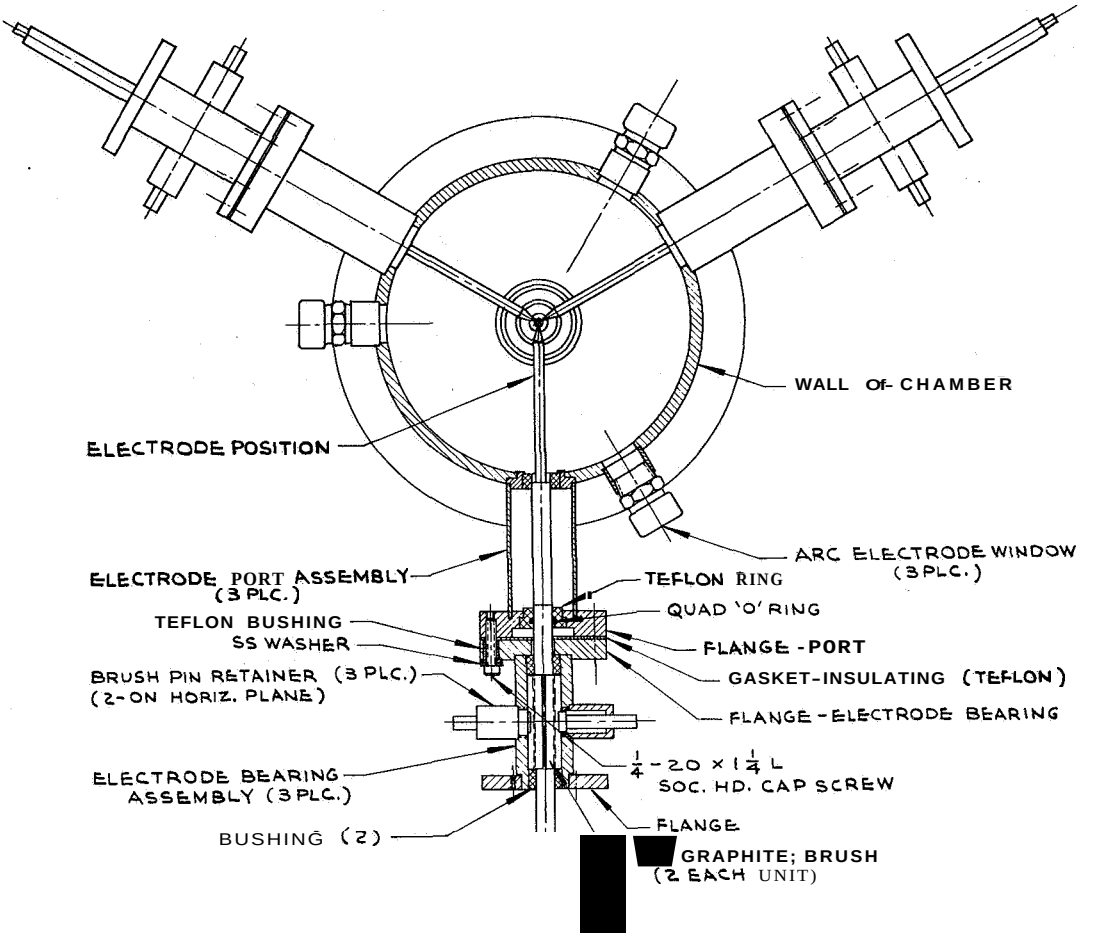

SECTION A – A

(ROTATED 30° COUNTER-CLOCKWISE)

FIG. 10 TOP SECTION VIEW OF ARC–VERNEUIL FURNACE MOD 2 ASSEMBLY SHOWING THREE HORIZONTAL ELECTRODES

the boule from each electrode is controlled by inserting or withdrawing the electrode, using a manually adjusted drive screw mounted outside the electrode assembly and not shown in Figs. 9 and 10. Two split copper–graphite brush segments are used to conduct current into each horizontal electrode. Copper–graphite sleeve bearings are used to support the electrode shafts and to maintain alignment during rotation. These are located on either side of the electrical brushes. Quad rings are used as sealing glands.

The horizontal electrode shafts are fabricated from stainless steel and graphite. The stainless steel section extends from outside the furnace through the brushes, bearings, and vacuum sealing gland. The horizontal electrode shafts are 1/2 inch in diameter, and the stainless steel section is followed by an intermediate section of high strength graphite (National Carbon Grade ATJ). Electrode tips are 1/4 inch in diameter and machined from spectrographic grade graphite. They recess into the ATJ graphite section. The furnace was designed to permit consumption of three inches of electrode length before a shut down for replacement of electrodes. Boron nitride sleeves surround each electrode as it enters the furnace chamber. These sleeves act as a secondary alignment guide for each electrode, and they ensure electrical insulation of the electrode and prevent particulate matter from entering the electrode housing. The boule holder and the furnace chamber are grounded. The horizontal electrodes and electrode support assembly were insulated from the remainder of the furnace using a Teflon gland and gasket.

A cylindrical graphite shield encloses the boule holder. This shield can be heated to 2300°C by radiation from a surrounding graphite resistance element, not shown in Figs. 9 and 10. This arrangement was designed to provide annealing of the boules or to permit slow cooling of the boules grown in the adjacent arc. Power for the resistance heater element is provided by a variable transformer with a rated output of 6 volts and 1500 amps. The radiation heater was designed to provide gradual cooling from temperatures above the lower temperature limit for plastic deformation, which is between 1825°C and 1925°C for polycrystalline tantalum carbide.[**] This was done to prevent the possibility of thermal stress cracking of tantalum carbide or hafnium carbide boules that cooled too quickly. However, as experimental data became available, it became apparent that tantalum carbide and hafnium carbide boules that were grown without the use of the radiation heater did not crack during cooling. Consequently, the radiation heater was not used for most of the crystal growing experiments.

The main chamber of the crystal grower, shown in Fig. 11, consists of (1) a bottom flange, (2) a lower cylindrical section surrounding the radiation heater and connected with a low impedence vacuum port, (3) an upper chamber housing the three horizontal electrodes and three windows, and (4) a top flange. The top flange provides for injection of feed powder and atmospheric gases. A modular assembly using O-ring seals and Vee-band couplers for rapid dismantling assists cleaning and loading.

Quartz windows, located on the same level as the horizontal electrodes, permit observation of the arc discharge to the molten cap of the boule at each electrode. These windows are sealed with O-rings and each is oriented 90° from a horizontal electrode. This arrangement permits the best practical view of each electrode and permits the operator to make the many small adjustments of electrodes required for successful growth of crystals. Optical filters are located outside the quartz windows for eye protection.

To aid the operator in more precisely controlling the elevation of the boule with respect to the horizontal plane of the electrodes, a convex objective lens was mounted at one window to project an enlarged image of the boule on a screen on which an orthogonal coordinate grid was superimposed. With the optical filter removed, this image was very intense, and dimming the room lights was not required. The top of each boule could be held within 0.2 mm of a predetermined optimum vertical position.

The particle feeder discharges into a carrier gas stream that conveys the carbide particles through a vertical injection tube to the molten cap. A double-walled, water-cooled, stainless steel tube with an inner diameter of 0.020 inch was used. The injection tube enters the furnace through a sealing gland in the center of the upper flange. An x-y horizontal positioning platen located above the furnace and below the powder feeder was used for the critical alignment of the injection tube with the boule.

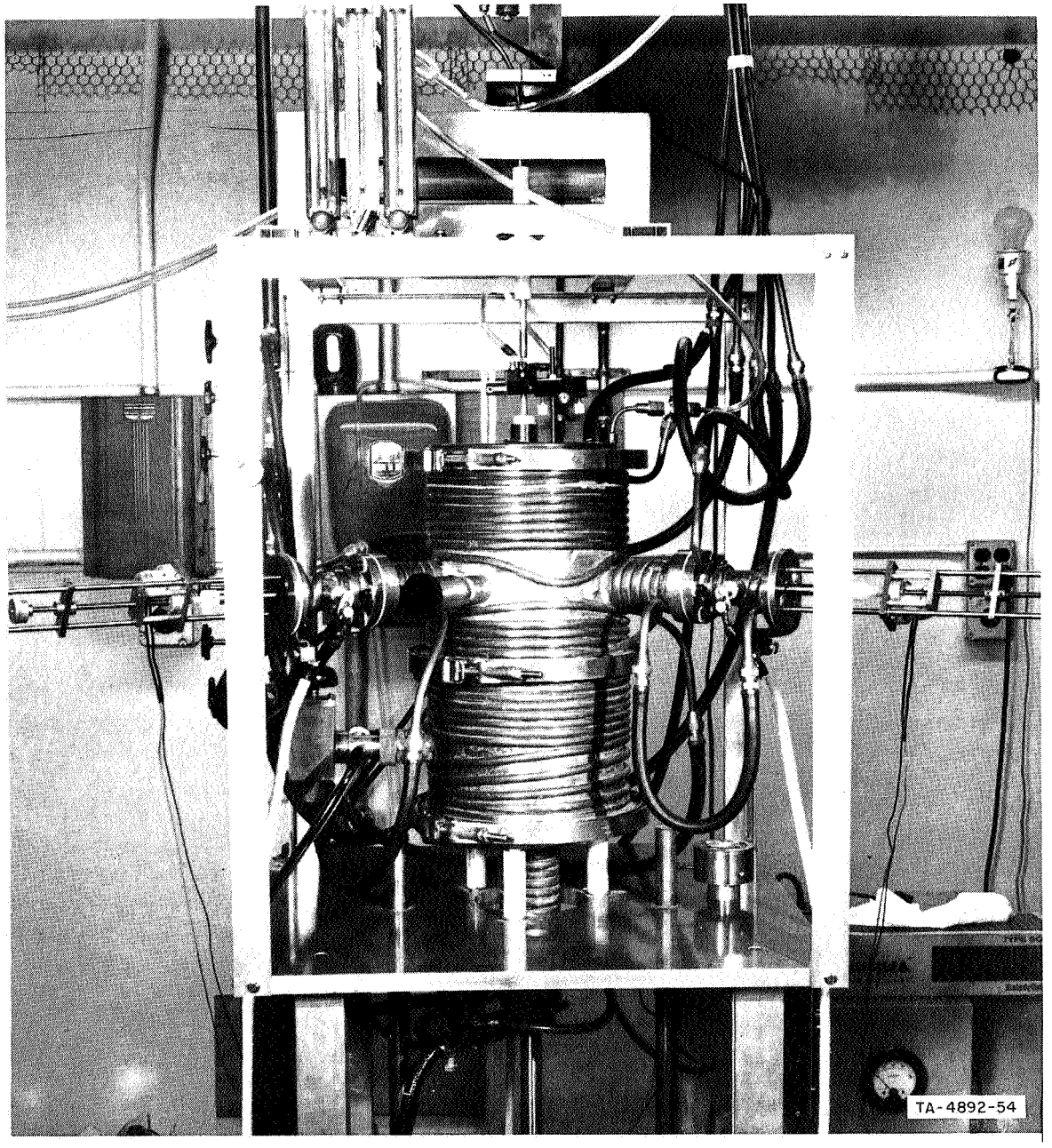

FIG. 11 ARC MELTING FURNACE FOR VERNEUIL CRYSTAL GROWTH

Particles are not melted or heated significantly before contacting the boule. This represents a significant difference from conditions in a conventional flame-fusion Verneuil process.

The injection tube stand-off distance from the molten cap, the particle size of carbide particle feed powder, and the carrier gas velocity are parameters that must be adjusted to prevent strong convection currents in the arc region from scattering the carbide particles before they reach the molten cap. High carrier gas injection velocities and relatively coarse particles were required because of the very intense turbulence in the arc region. A number of tantalum carbide particle sizes were tried and a fairly coarse particle size fraction, -200 + 270 mesh, was found to be optimum. Restricting the inside diameter of the injection tube also reduces the amount of particle dispersion and increases the percentage of the powder feed that reaches the boule. The original 0.040-inch ID injection tube was too large. Particles within the injection tube are accelerated, by the carrier gas, to velocities much greater than their terminal settling velocities.

The powder feeder, located above the crystal growth furnace, is sealed to prevent gas leaks during evacuation of the furnace chamber. A variety of feeders have been tested, but none have been completely satisfactory for controlling the flow of these powders. The results of feeder tests are summarized in Table 111. A Metco feeder* and a capillary tube centrifugal device, designed at the Institute, gave satisfactory performance. The feeder problems are difficult because of the high specific gravity, coarse particle size, and free flowing characteristics of the powder. Very slow feed rates are necessary for crystal growing. The desired properties of the feeder are a continuously variable feed rate from a small value down to zero and a reproducible relationship between the controller setting and the feed rate. Powder feed rates were lowered by using a short cycle timer with an adjustable on and off period during each cycle to control the feeder. Intermittent operation did not adversely affect crystal growth so long as the cycle did not exceed one minute.

* Metco Inc., Westbury, New York

Table III

SUMMARY OF EXPERIENCE WITH PARTICLE FEEDERS IN MELT GROWTH OF REFRACTORY CARBIDES

FEEDER	OPERATING PRINCIPLES	DESIGN	RATING	MAJOR DIFFICULTIES
Metco MP	Particles settling to the bottom of the feeder are aspirated into the main gas carrier stream by a small cross-current jet of carrier gas. Particle movement is increased by vibrating the feeder. System designed for coarse particles (+325) used in plasma spraying.	Commercial	Marginal	Poor reproducibility of flow rate
Centrifuging, upturned capillary	Settling particles enter a neck and capillary. The capillary is upturned at an angle θ from the horizontal so the particles must travel up an inclined plane. The powder reservoir with capillary is rotated about its vertical axis. Particles flow when centrifugal forces exceed gravitational forces. This condition is satisfied when $v_t^2/r \geq g \tan \theta$. Since $v_t = 2\pi r \Omega/60$, where Ω is the rotary speed of the feeder in rpm, the critical speed (Ω_c) in rpm for particle flow is $\Omega_c > (60/2\pi)\sqrt{rg \tan \theta}$.	SRI	Marginal	Oversize particles occasionally clogged feeder, requiring a high rotation speed to release the particle. This led to an unsatisfactory burst of excess carbide.
Mechanically vibrated sieve feeder	Particles pass through sieve. Rate depends on vibration intensity.	Commercial	Unsatisfactory	Cake of particles were too free flowing
Audio pulsed gas column sieve feeder	Particles pass through sieve; rate influenced by pulsing gas column driven by a low frequency audio speaker.	SRI (MIT-Insulation Laboratory concept)	Poor	Used very small open area in sieve to overcome free-flowing tendency of particle, but feed rate varied with damping mass of particles covering the screen. The high density of TaC restricted the powder loading. Short operating period before reloading.
Blade chopper	An ultrathin slice of a compacted mass of particles is removed on each cycle by a rotating blade. Feeder designed for fine particles that will hold together as a quasi-free standing body.	SRI	Unsatisfactory	Particle size too large for effective compaction.

A matching single phase power supply was built for the crystal grower. A step-down transformer was followed by three saturable core reactors, one for each horizontal electrode. The maximum output of the power supply is 35 volts; however, operating voltage is normally determined by the arc impedance. Each saturable reactor has a continuous duty limitation of 250 amp. Current output is adjustable from approximately 50% to 100% of maximum output.

Gas mixtures added to the furnace are controlled with flow meters. During a crystal growth experiment, constant injection of carrier gas and flow from the furnace chamber is required. A diagram of the power circuit and gas flow circuit is given in Fig. 12. One of the flow meters provides for direct argon inlet into the chamber. The other two flow meters provide for metering and mixing hydrogen and argon used as the carrier gas stream in the powder injection tube. The gas outlet train provides for high vacuum pumping with a filter to trap particulate matter and a vacuum pump bypass for purging at 1 atm. Pumping through the filter is usually employed until the furnace chamber is evacuated to a few torr, at which point the filter is bypassed to decrease pump impedance and thoroughly evacuate the chamber.

D. Operating Procedures

Early in the program, growth of tantalum carbide and hafnium carbide single crystals was initiated on hot pressed carbide seeds and on single crystal seeds. However, thermal stresses associated with starting the arc often fractured seeds and prevented completion of runs.

The most successful technique uses as a seed a short tantalum rod, approximately 1/2 inch long by 1/8 inch in diameter. The rod is placed in a hole recessed in the graphite pedestal. When the arc is initiated, the tantalum melts back to the graphite pedestal, forming a liquid pool. As carbide powders are dropped onto the surface of the pool and are slowly cooled, a strong weld results. Boules started in this manner initiate as polycrystalline rods and depend on the dominance of a well-oriented crystallite to occupy the major portion of the growing boule and eventually exclude all other crystals. An example of a tantalum carbide boule grown in this manner is shown in Fig. 13.

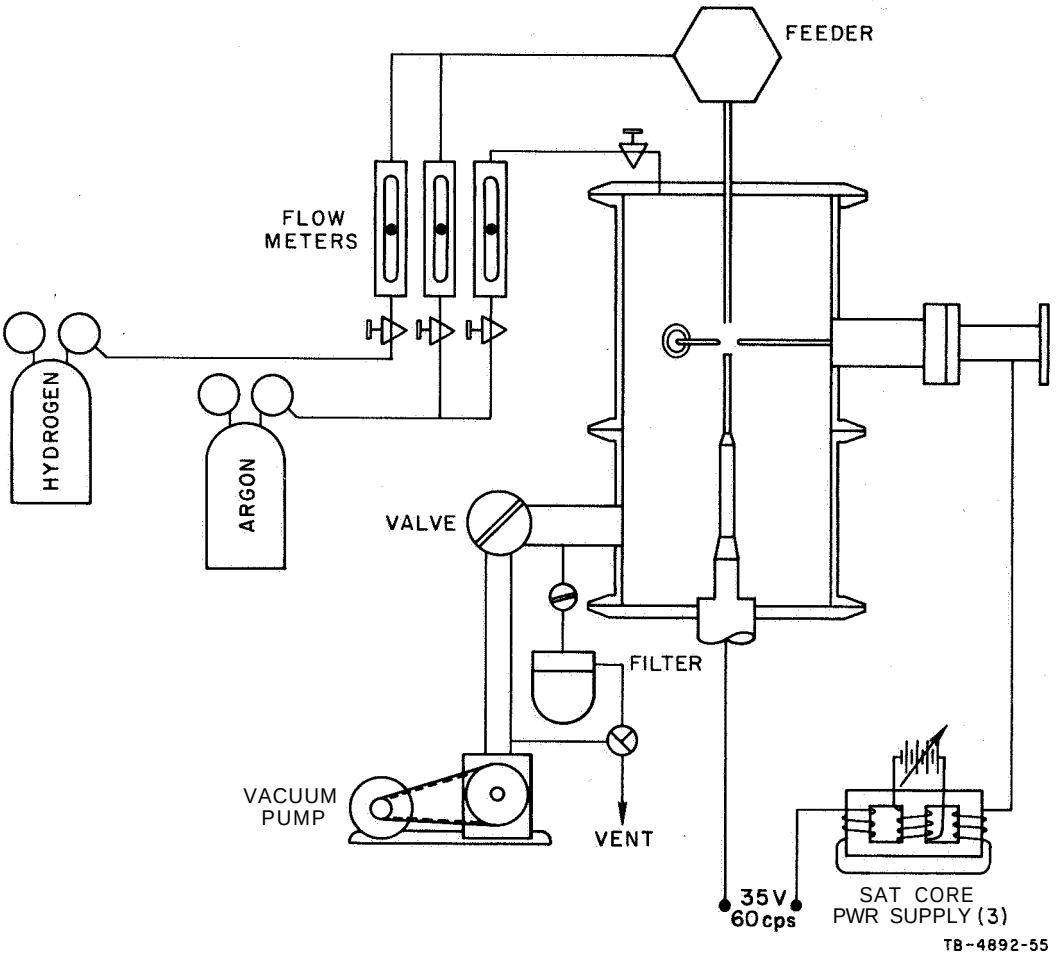

FIG. 12 POWER AND GAS CONNECTIONS FOR ARC–VERNEUIL FURNACE

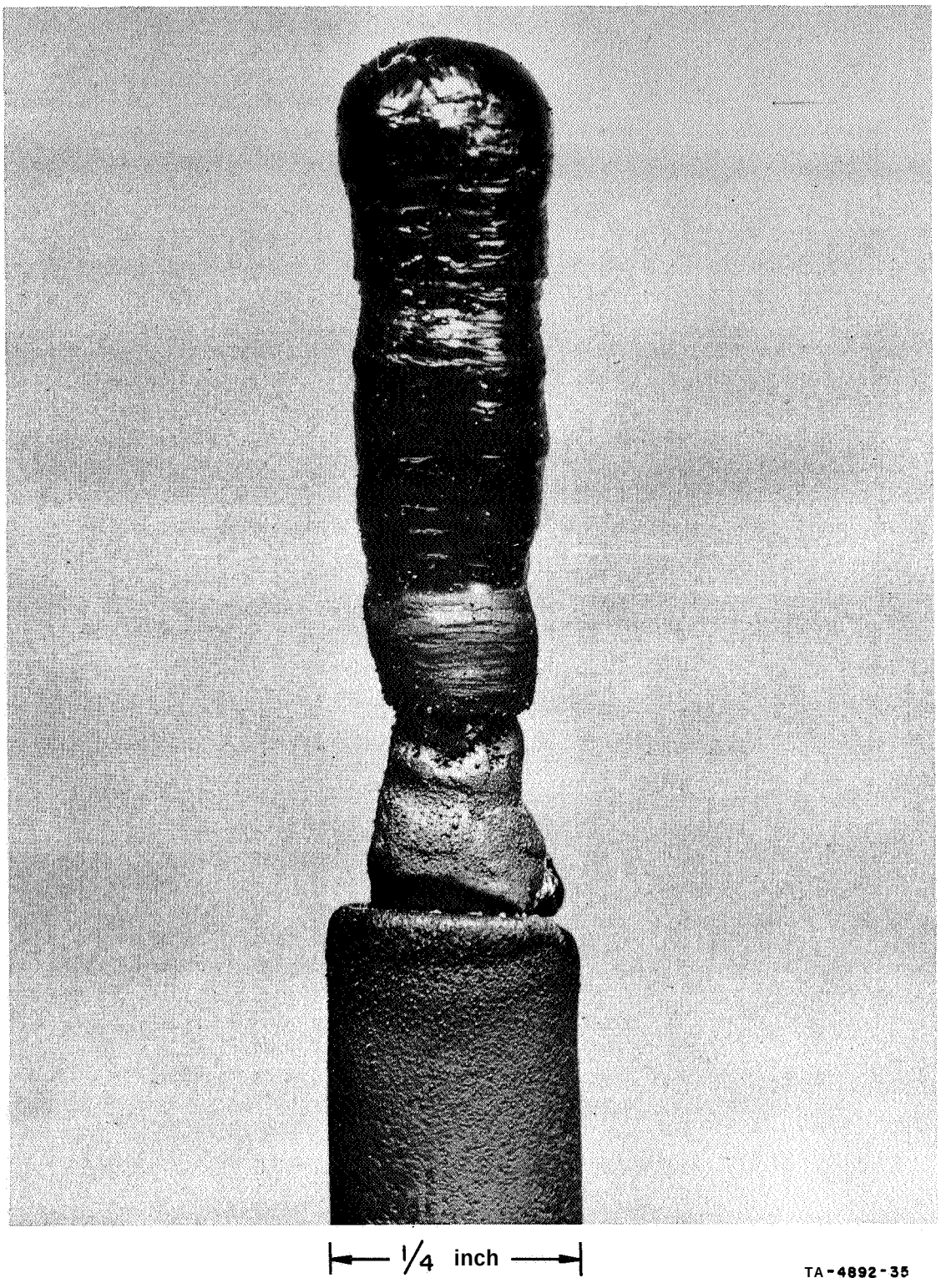

FIG. 13 SHORT TANTALUM CARBIDE BOULE ($TaC_{0.9}$) GROWN IN THE ARC–VERNEUIL FURNACE

A crystal growth run is initiated by evacuating and refilling the furnace chamber with an inert or protective gas mixture. For tantalum carbide, the optimum environment is a 5% to 10% hydrogen in argon at a total pressure of 0.5 to 1 atm. For hafnium carbide, the optimum environment is 100% argon at 1 atm.

The arcs are started and adjusted, with all the electrodes rotating, before the particle feeder is started. A molten cap is established, and as the boule grows it is slowly lowered into the annealing chamber. Elevation of the molten cap must be carefully controlled. Too high an elevation leads to a pinch-off effect in which a thin neck of solid carbide grows up from the center of the boule. Ideally, the top of the liquid meniscus of the melt is maintained at or below the center line of the horizontal electrodes. A full hemisphere of molten carbide is maintained to prevent crystal nucleation at the side of the boule.

It is very important that the electrodes and boule holder be manipulated to prevent eccentricity of the boule with respect to the rotation axis. Power inputs from each of the three electrodes must be kept reasonably equal by carefully controlling and monitoring the electrode gap. The horizontal carbon electrodes should be blunted and maintained within 1/16 inch of the boule.

The effect of the speed of rotation of boules during crystal growth was systematically studied. Some rotation is required to distribute heat evenly and to compensate for any eccentricity in the deposition of particles on the boule. At excessive rotation speeds, a centrifugal oscillation or apparent whipping of the boule causes it to become eccentric with respect to the axis of rotation. The best rotation speed for 1/4-inch-diameter boules is 10 to 16 rpm.

For best results, all -325 mesh and +200 mesh particles must be removed from the feedstock by screening. To obtain good single crystal sections, relatively long boules, usually greater than 2 inches, are required and they should be grown at much faster rates (5 to 10 cm/hr) than are typical for conventional Verneuil crystal growth.

Boule growth is terminated at 3 inches unless operating difficulties have necessitated earlier termination. Power is turned off immediately and the boule is cooled rapidly to prevent further decarburization of tantalum carbide. The cap of each boule, which is polycrystalline because of rapid solidification, is removed. The remaining upper one inch of the boule normally provides the larger grains or single crystal sections, suitable for cutting single crystal specimens.

E. Summary of Results

Boules of tantalum monocarbide, hafnium monocarbide, and mixed solid solutions were grown in the arc-Verneuil apparatus. Elimination of grain boundaries was the major difficulty encountered for each carbide. This problem is discussed in greater detail in Section III-F. Analyses of starting materials and crystals are given in Section VI.

1. Tantalum Carbide

Using 5-10% hydrogen in the carrier gas yielded single phase tantalum monocarbide boules with bulk carbon contents between 43 and 46 at.%. Attempts to raise the carbon content further by using other additions to the gaseous environment or the starting powder were unsuccessful.

These boules had a recarburized zone near the surface less than 0.001 inch thick which forms on the solid boule as it cools through an intermediate temperature zone where recarburization in the presence of the highly carburizing environment is thermodynamically favored. This high-carbon surface layer, which is usually yellow (>46 at.% carbon), overlays a 0.001- to 0.005-inch zone of very low carbon content, usually containing Ta_2C. This inner layer is formed by carbon depletion from the solid at a temperature near the melting point. Thus, the variation in carbon concentration near the surface of tantalum carbide boules results from solid state diffusion of carbon and is a natural consequence of the time-temperature history of the boule during cooling. When hydrogen is used to prevent excessive decarburization of the bulk tantalum carbide, these surface zones are of superficial thickness and make a negligible contribution to the average carbon content of the boule. When boules are sectioned by diamond sawing, this surface material is removed.

About 10% of the tantalum carbide boules were sufficiently free of secondary grains to yield single crystal bars longer than 0.4 inch after cutting. A few single crystal bars one inch in length were obtained.

2. Hafnium Carbide

As the vaporization data in the literature suggested, no difficulty was encountered in maintaining a high carbon composition in growing hafnium carbide boules. However, the higher total vaporization pressures and rates resulted in slightly smaller diameter hafnium carbide boules than tantalum carbide boules. More importantly, the first hafnium carbide boules grown were extremely porous. This resulted from operating at chamber pressures too low to prevent bubbles from forming within the molten cap. Dense hafnium carbide boules could not be grown at pressures below 1 atm.

The variation in grain size was similar to that observed in tantalum carbide, with a poorer distribution of large grains. Obtaining high purity starting powders in the desired particle size range was extremely difficult, and the poor powder quality is believed to account for many of the nucleation problems encountered.

3. Mixed Solid Solution Carbides

Homogeneous single phase boules were grown from homogeneous solid solution carbides that were formed by carburizing particles of a solid solution Hf-Ta alloy. Starting powders of two compositions were employed: 80 at.% TaC/20 at.$ HfC and 60 at.$ TaC/40 at.% HfC. The general behavior of these carbides during crystal growth was similar to that of tantalum carbide. Although some carbon was lost, as Fig. 7 shows, carbon vaporization was not a serious problem.

All the boules were polycrystalline with grains too small to permit cutting single crystal sections larger than 1 mm. Attempts to grow mixed solid solution boules by feeding discreet tantalum carbide particles physically mixed with discreet hafnium carbide particles resulted in multiple diffraction peaks and spreading of the diffraction peaks.

These results indicate that the boules were nonhomogeneous and that homogeneous solid solution carbide crystals could only be grown by starting with feed particles that are also homogeneous.

F. Grain Boundaries and Subgrain Boundaries in Arc-Verneuil Boules

1. Grain Boundaries

As has been mentioned above, inability to eliminate grain boundaries was the major obstacle to growth of satisfactory single crystals. The largest boundary-free sections were obtained with tantalum carbide. On the average, the mixed carbides have been slightly finer-grained than tantalum carbide or hafnium carbide. However, there are considerable differences between several boules of the same material. Grains tend to be columner with the growth direction. The smaller grains are eliminated during formation of the boule by a gradual expansion in cross section of the dominant grains, in the classical manner for flame fusion crystal growth. However, new grains are occasionally nucleated at or near the surface and internally. In cross section, the surface grains appear as isolated semicircles, and the internally nucleated grains appear as a broad root spreading out from the nucleation point as the grain grows upward. The initial tip of an internal grain nucleated in a hafnium carbide boule is shown in Fig. 14. This new grain grew to be about 1/8 inch across.

There is no obvious relationship between impurity content and grain size of boules. Large grains were obtained with hafnium carbide, one of the least pure starting powders. Good boules have been obtained from collected excess hafnium carbide powder put through the crystal growing furnace a second time without being cleaned after the first run. No evidence of impurity segregation at grain boundaries or grain boundary nodes could be detected by electron beam microprobe analysis.

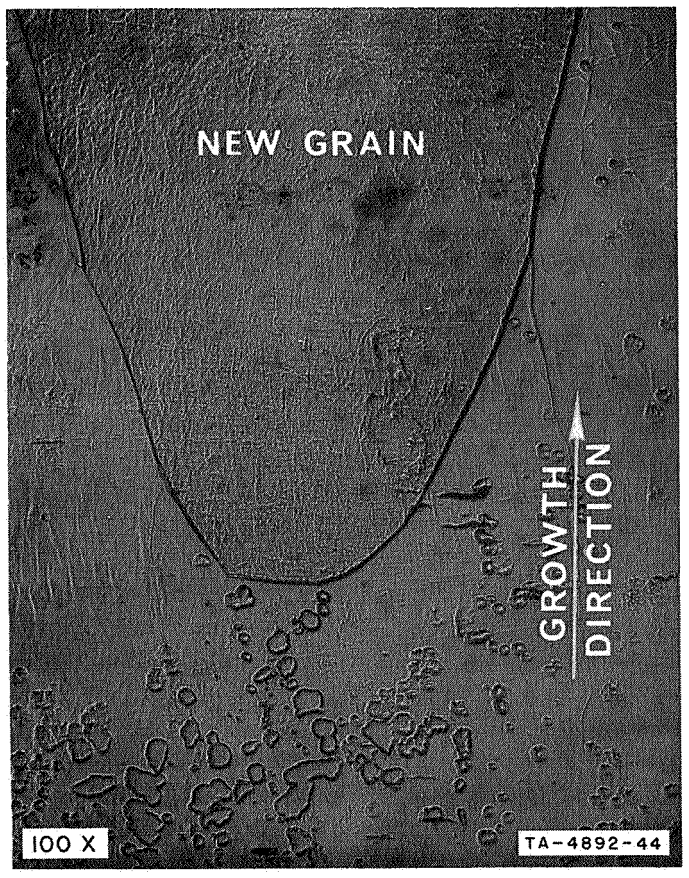

FIG. 14 NUCLEATION REGION FOR GROWTH OF NEW GRAIN IN HAFNIUM CARBIDE (100X)

Further studies aimed at identifying the source of nucleation in new grains included an investigation of particle intrusion into the liquid cap. Studies of boule cross sections were made to secure information on the configuration of the liquid cap and any evidence of incomplete melting of carbide particles. When the arc discharge is terminated during crystal growth, the molten cap quickly solidifies. A fine-grained structure results that contrasts sharply with the coarse-grained or single crystal boule below the molten cap. The change in grain size indicates the location of the liquid/solid interface when the arc is quenched. On this basis, molten caps on 1/4-inch-diameter boules are judged to be 1 to 2 mm deep. A photograph of a typical quenched cap is shown in Fig. 15.

There has been no metallographic evidence of carbide particles being trapped in the boule without melting. Nevertheless, nucleation of new grains may be caused by carbide particles settling to the liquid/solid interface before melting or dissolving in the liquid carbide cap. These particles could act as nuclei for growth of new grains and would not appear in their original size when the boule is cross-sectioned. This problem may be increased when a carbon-deficient molten tantalum carbide cap is present with a lower liquidus temperature than the melting point of the stoichiometric carbide particle, A series of growth experiments using different particle sizes, but in all other respects identical, was conducted to determine if there was a relationship between particle size employed in Verneuil growth and subsequent grain size of the boule that could be related to nucleation of new grains by unmelted particles. Particle sizes of -200 +270 mesh, -270 + 325 mesh, and -325 mesh were used. The tests with both hafnium carbide and tantalum carbide show no systematic variation in grain size with particle size in the feeder.

Particle velocities on impact with the molten cap were estimated from the velocity and Reynolds number of the gas flowing within the injection tube. Particle penetration distances into the molten cap before a reduction in particle velocity to insignificant levels were also estimated using a computer program. The results indicate that particles in

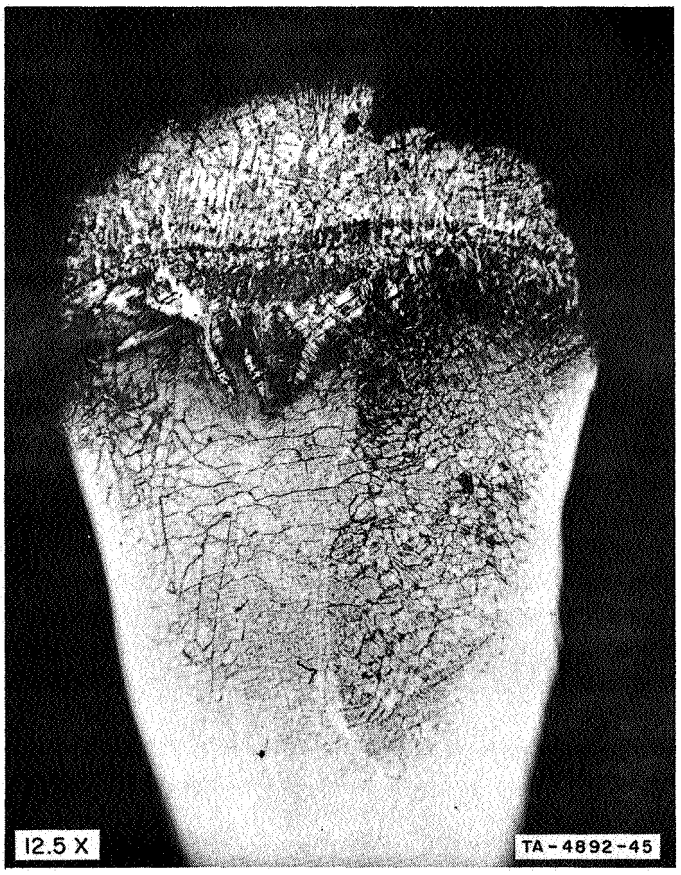

FIG. 15 CROSS SECTION OF TANTALUM CARBIDE BOULE INDICATING REGION OF MOLTEN CAP (12.5X)

the size range used in our crystal growth experiments are not likely to penetrate through the molten cap and nucleate a new grain before melting.

2. Subgrain Boundaries

Subgrain boundaries usually appear after polishing and etching tantalum carbide and hafnium carbide crystals. An example of heavy intrusions of subgrain boundaries in tantalum carbide is shown in Fig. 16. In this photograph, primary grain boundaries outlining seven grains can also be seen. Although there is no sure way to distinguish grain boundaries from subgrain boundaries except by X-ray diffraction procedures, which were used extensively, the primary grain boundaries do appear in the diamond cut surface before polishing, whereas subgrain boundaries are only revealed by polishing and suitable etching.

Individual dislocation etch pits can be seen within tantalum carbide subgrain boundaries at higher magnification in Fig. 17. This photograph shows a primary grain boundary traversing from the upper left to the lower right quadrant, with several subgrain boundaries intersecting it.

Etched surfaces of tantalum carbide were replicated to secure electron micrographs of dislocation etch pits in subgrain boundaries of tantalum carbide at still higher magnifications. The electron micrograph in Fig. 18 shows a typical array of dislocation etch pits in the subgrain boundary intersecting a (100) face. In this instance, the linear dislocation density is approximately 3×10^4 dislocations per centimeter, corresponding with a tilt boundary of about 0° 12'.

In hafnium carbide, subgrain boundaries often appear to end abruptly within the boule. In other instances the depth of etching often changes abruptly along the subgrain boundary. Examples of subgrain boundaries in hafnium carbide single crystal sections are shown in Fig. 19.

FIG. 16 ETCHED $TaC_{0.9}$ WITH GRAIN BOUNDARIES AND SUBGRAIN BOUNDARIES (50X)

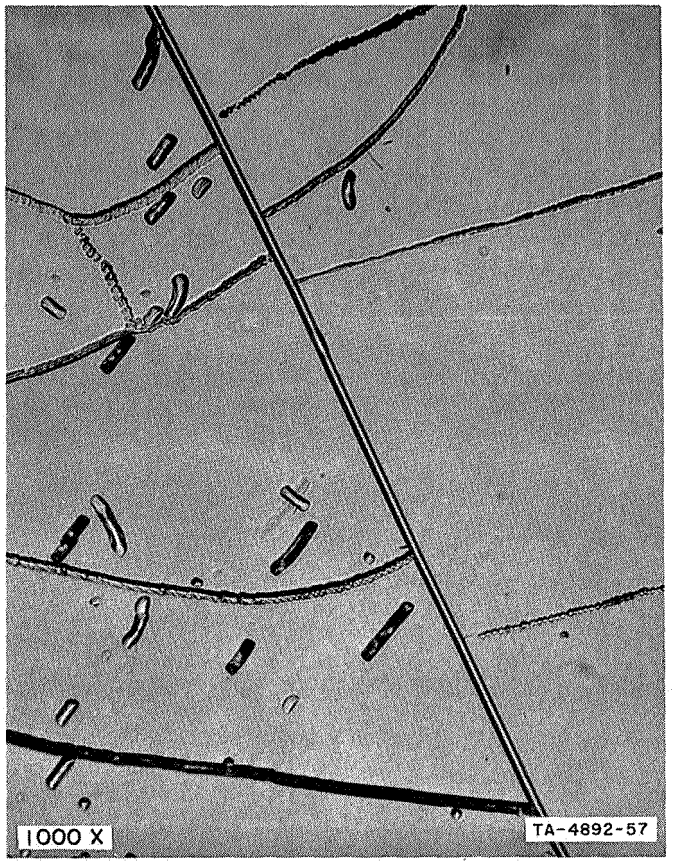

FIG. 17 ETCHED $TaC_{0.9}$ WITH GRAIN BOUNDARY AND SUBGRAIN BOUNDARIES (1000X)

FIG. 18 DISLOCATION ETCH PITS IN $TaC_{0.9}$ SUBGRAIN BOUNDARY

FIG. 19 SUBGRAIN BOUNDARIES IN SINGLE CRYSTAL OF HAFNIUM CARBIDE (1500X)

G. Arc Stability and Gas Composition in Melting Tantalum Carbide

The problems encountered in maintaining stable crystal growth conditions in the arc increased with increasing additions of hydrogen to the furnace environment. At high hydrogen contents, nearly all runs were terminated by extinguishment of the arc or by failure to maintain proper melting conditions. Since an increase in the carbon content of tantalum carbide boules was desired, attempts to stabilize the arc in higher hydrogen mixtures and to secure other more effective gaseous environments were made. These efforts included experiments with a high frequency, high voltage arc-stabilizing circuit, additions of NaCl to the powder feed stock in order to improve the arc conductivity, substitution of freon (F_2CCl_2) for hydrogen, and additions of excess graphite powder to the feed stock.

1. Arc Stabilizing Circuit

In principle, a high frequency arc-stabilizing circuit can be superimposed on the low frequency power supply circuit of the crystal growing furnace without affecting the low frequency circuit function. A high frequency power supply at high voltage can ensure that the arc will not extinguish under marginal operation conditions. A comparatively large high frequency and high voltage generator is required to overcome the parasitic capacitance of the electrode holder (160 picofarads). A BC-610 E radio transmitter capable of operating at 350 watts was adapted for use at a frequency of 2 megaHertz to stabilize one of the three horizontal electrodes of the crystal growing furnace. The circuit diagram is shown in Fig. 20. With this power supply, the high frequency voltage drop across the arc was approximately 200 volts. This was not a significant improvement over the 30-volt potential imposed by the low frequency main arc power supply and was only of marginal value in stabilizing the arc plasma. After installation, the BC-610 E generator was used for the growth of several tantalum carbide boules. Eventually its use was discontinued because of its marginal effect on crystal growth.

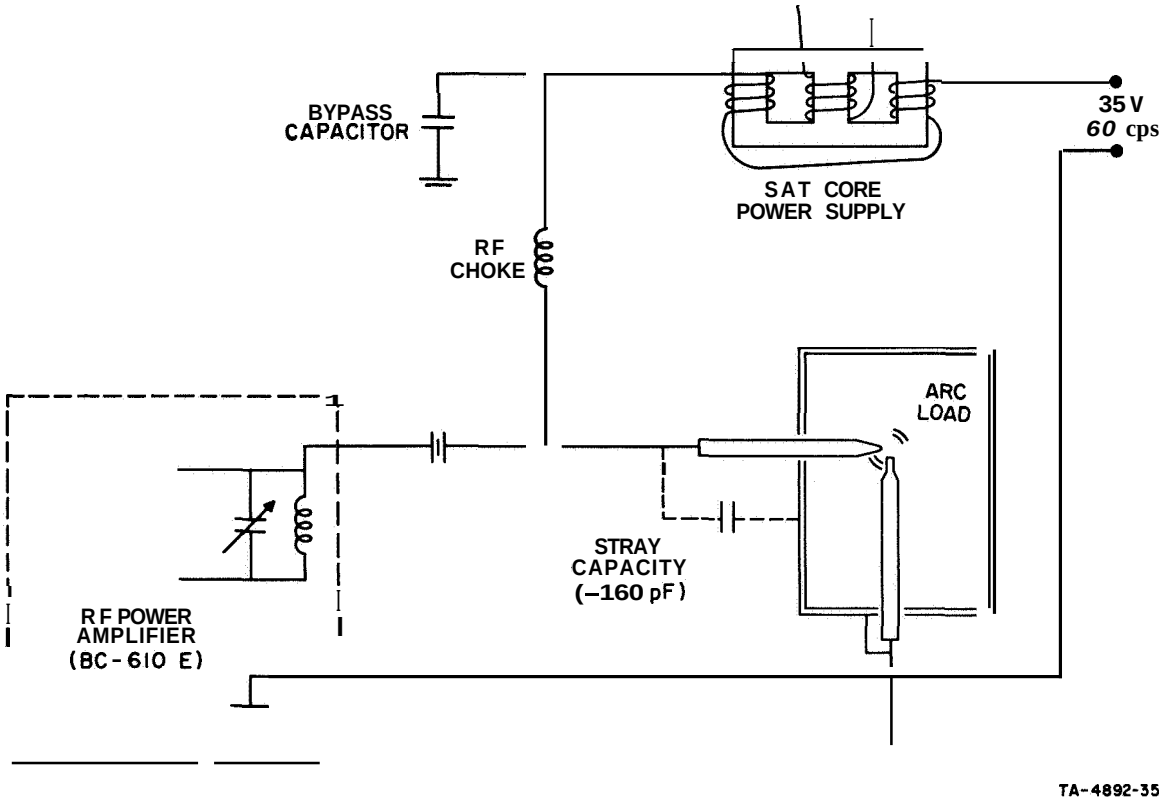

FIG. 20 CIRCUIT FOR SUPERIMPOSING A HIGH FREQUENCY STABILIZING SIGNAL ON THE ELECTRODE

2. NaCl Additions

Two crystal growth experiments were conducted in which a mixture of 50 wt % hafnium carbide and 50 wt % sodium chloride powders were fed onto a growing boule. The purpose of these experiments was to determine what effect chlorine has on the vapor transfer of hafnium away from the boule and to determine if seeding the arc plasma with a source of sodium vapor, which is easily ionized, has any effect on the stability of the arc. Sodium chloride did not affect the stoichiometry of the hafnium carbide boules resulting from these experiments. Because of the small plasma volume of the arc region and the discrete injection of NaCl particles, it was not possible to maintain a continuous presence of sodium vapor in the arc. Consequently the use of sodium chloride had no lasting effect on stabilizing the arc and further use was discontinued.

3. Freon (F_2CCl_2) Environment

Five tantalum carbide crystal growth experiments were conducted in gaseous freon (F_2CCl_2) and freon-argon gas mixtures to investigate the feasibility of using freon to replenish carbon vaporized from the boule without introducing H_2 and H radicals into the plasma. These experiments showed that freon cannot be used to sustain an arc-plasma and that freon quenches argon plasmas as readily as hydrogen does. Arc stability could not be maintained unless the freon content of the gas was less than 5%. Carbon content of tantalum carbide boules was not significantly affected by this amount of freon when compared with 10% hydrogen in argon. Lattice parameter measurements indicate that the carbon content of boules grown with 5% freon is about 43 at.%.

4. Graphite Powder Additions

Boules were also grown using a particle feed mixture of tantalum carbide and graphite powders in an attempt to improve the carbon ratio of the resulting crystals. Crushed graphite, -270 +325 mesh, was mixed with tantalum carbide powder. No improvement in the carbon content of the boules resulted from these tests. Because of the low density and slow settling rate of the graphite particles, very few of them may have come in contact with the boule. Flow meters were changed to permit more rapid flow of gas through the injection tube carrying feed particles to the boule, but this did not affect the carbon content. Since no improvement in the carbon stoichiometry was obtained in these experiments, crystal growth studies employing mixtures of graphite and tantalum carbide were discontinued.

H. Related Experiments

A number of additional experiments were made in which operating procedures were varied considerably in attempts to either reduce the number of grain boundaries obtained or increase the carbon content of tantalum carbide boules.

Graphite heat shielding. In an attempt to retard preferred vaporization of carbon from tantalum carbide, the surface area of hot carbon surrounding the boule was increased. This was done by using larger electrodes and using a pyrolytic graphite heat shield. The horizontal electrode diameter was varied between 1/4 inch and 1/2 inch. Power fluctuations caused frequent overloads and circuit interruptions when the 1/2 inch electrodes were used. Boules made with 1/2 inch electrodes were slightly larger in diameter, but no improvement in their carbon stoichiometry was obtained.

Experiments were made with a pyrolytic graphite heat shield that consisted of a 2-inch diameter, thin-walled dome surrounding the boule as shown in Fig. 21. Each of three windows cut in the side walls of the heat shield allowed entrance of one electrode and provided a view of one of the alternate electrodes. Observation of electrodes was required to control their stand-off distance. The heat shield rested on an insulating boron nitride platform that was attached to the seed holder. When the seed was rotated, the heat shield also rotated until the horizontal electrodes came in contact with the sides of the windows, which prevented further rotation. This sequence aligned the heat shield window with respect to the outer observation ports of the furnace. A few short boules were grown using this heat shield, but they did not have carbon contents above 46 at.%. During crystal growth, the inside surface of the heat shield had a brightness temperature of 2300°C while the outside surface brightness temperature was 1650°C. These temperatures were probably insufficient to have a significant effect on the crystal growth process.

Solid state diffusion of carbon in Tantalum Carbide. Some experimental studies were undertaken to increase the carbon content by a post-growth treatment. Boules grown earlier in this investigation that had been cross sectioned longitudinally and showed evidence of Ta_2C precipitation were cross sectioned in the transverse direction to provide wafers approximately 1/16-inch thick. Wafers were surrounded with graphite powder and subjected to diffusion anneals at 2000°C in argon

and vacuum. Although the rate of diffusion of carbon in TaC_{1-x} at this temperature was expected to be very slow, the amount of carbon needed to compensate for the Ta_2C was also very small. The results of a 24-hour test at 2000°C showed that Ta_2C had been removed from most of the polycrystalline TaC wafer. The diffusion experiments indicated that it would be possible to back diffuse carbon in carbon-deficient tantalum carbide. However, this step may generate additional imperfections in the crystal.

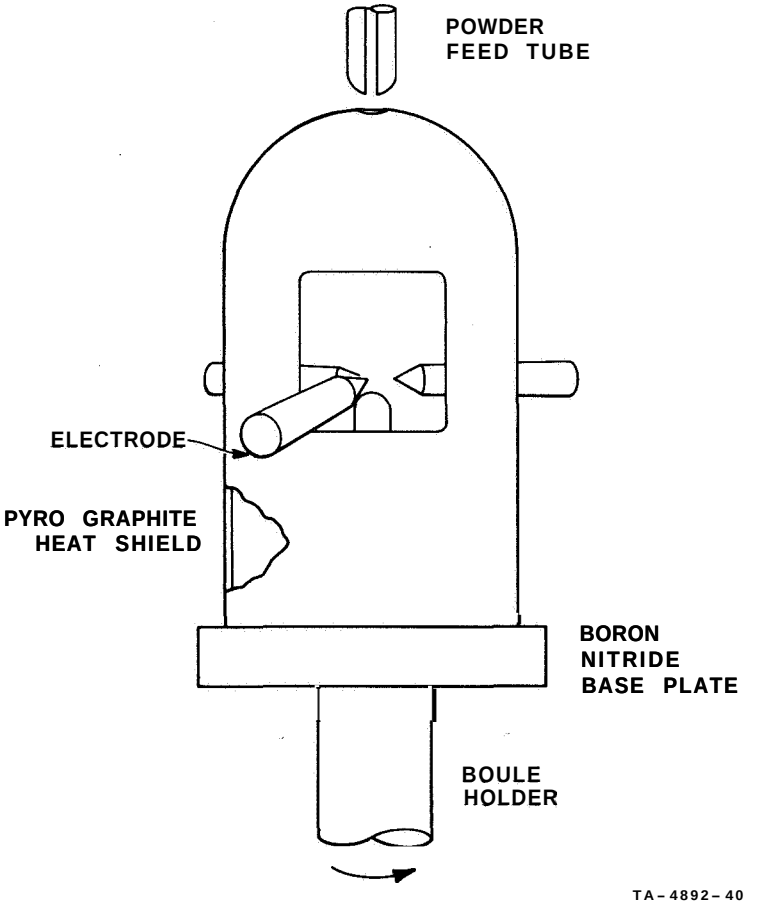

FIG. 21 PYROLYTIC GRAPHITE HEAT SHIELD

Float zone experiments. The arc-Verneuil furnace was temporarily modified to permit floating zone refining experiments using the horizontal electrodes for melting a zone of refractory carbide. A Materials Research Corporation zone refiner, in the vertical orientation, was mounted above the arc-Verneuil apparatus in place of the powder feeder normally used for Verneuil fusion experiments. An extension arm from the boat carriage of the zone refiner entered the top of the arc-Verneuil furnace through the seal normally used for the powder feed tube. Inside the furnace, a 0.125-inch-diameter tantalum rod was connected to the zone refiner extension arm by an appropriate chuck. This arrangement, used in conjunction with the existing arc-Verneuil apparatus, permitted independent vertical motion at variable rates as well as independent rotation at variable rates for both the upper and lower sections of a zone refined "ingot." The upper section consisted of a tantalum carbide boule or hot-pressed billet attached to the tantalum rod. The lower section was a tantalum carbide boule or hot-pressed billet inserted in the graphite seed holder. In principle, melting could be initiated in the center of a sample supported at both ends, or the separated upper section could be brought in contact with the lower section after striking the arc.

The results of six experiments are summarized in Table IV. In some cases, melting of tantalum carbide and attachment of the tantalum carbide rods were achieved. However, the arc tended to discharge to the lower (grounded) section with the result that attachment was hard to maintain and the operation was highly unstable. The resulting samples were small and very irregular. Also, a decrease in the number of grain boundaries was not obtained. Consequently, further experiments of this type were not attempted.

Table IV

SUMMARY OF ARC-FLOAT ZONE EXPERIMENTS

Run Number	Bottom Section	Top Section		Atmosphere (15 psia)	Results
1	TaC boule	Hot-pressed TaC billet		Argon	The top section would not melt, but small pieces of it were dislodge by the rotating boule. These fell into the boule.
2	HfC boule	Hot-pressed HfC billet	Ye	Argon	Similar to run 1.
3	TaC boule	Hot-pressed TaC billet		Argon	Melting and joining was established. The liquid was moved up and down by vertical translation of the sample.
4	Ta rod (0.125 in.)	Ta rod (0.125 in.)		90% Argon-10% Hydrogen	The rod melted in the center and parted into the upper and lower sections.
5	Ta recessed in the graphite seed holder	Hot-pressed TaC billet		Argon	The TaC billet was drip-melted onto the hot pedestal where a boule formed similar to arc-Verneuil growth.
6	Ta recessed in the graphite seed holder	Hot-pressed TaC billet		Argon	The billet was joined to the seed holder and quickly lowered. The sample parted to leave a small lower boule.

IV MELT GROWTH BY INDUCTION PLASMA HEATING

A. Apparatus

An induction-coupled plasma torch [..] has several advantages as a heat source for Verneuil growth of crystals. Very high temperatures are attained in the plasma; there are no electrodes or other components that must be heated to high temperatures; and a wide range of gas compositions can be used.

A sketch of the R-F plasma heated crystal grower constructed at Stanford Research Institute is shown in Fig. 22. The plasma tube shown in the upper part of the figure has a double wall construction to permit water cooling and is flared at the base to permit a gas-tight seal to the lower furnace chamber. This tube was initially constructed of Pyrex but subsequent operations caused thermal stress cracking of this tube at high power levels and quartz was substituted. In order to eliminate catastrophic stresses which can arise due to different expansion levels of the two wall during operation, the walls of the plasma containment tube were not joined at the top.

Immediately below the plasma tube is a resistance heated carbon furnace operating well above the minimum temperature for plasticity in the refractory carbides. This furnace was employed to maintain the desired temperature distribution during growth as well as to permit crystals to cool slowly at the completion of a run. Two R-F power supplies were used. The principal one was a 20-kw tuned-grid, tuned-plate unit constructed at Stanford Research Institute and tuned for maximum stability at 5.5 megaHertz. High-power experiments utilized a 50-kw Lepel generator operating at 5.0 megaHertz.

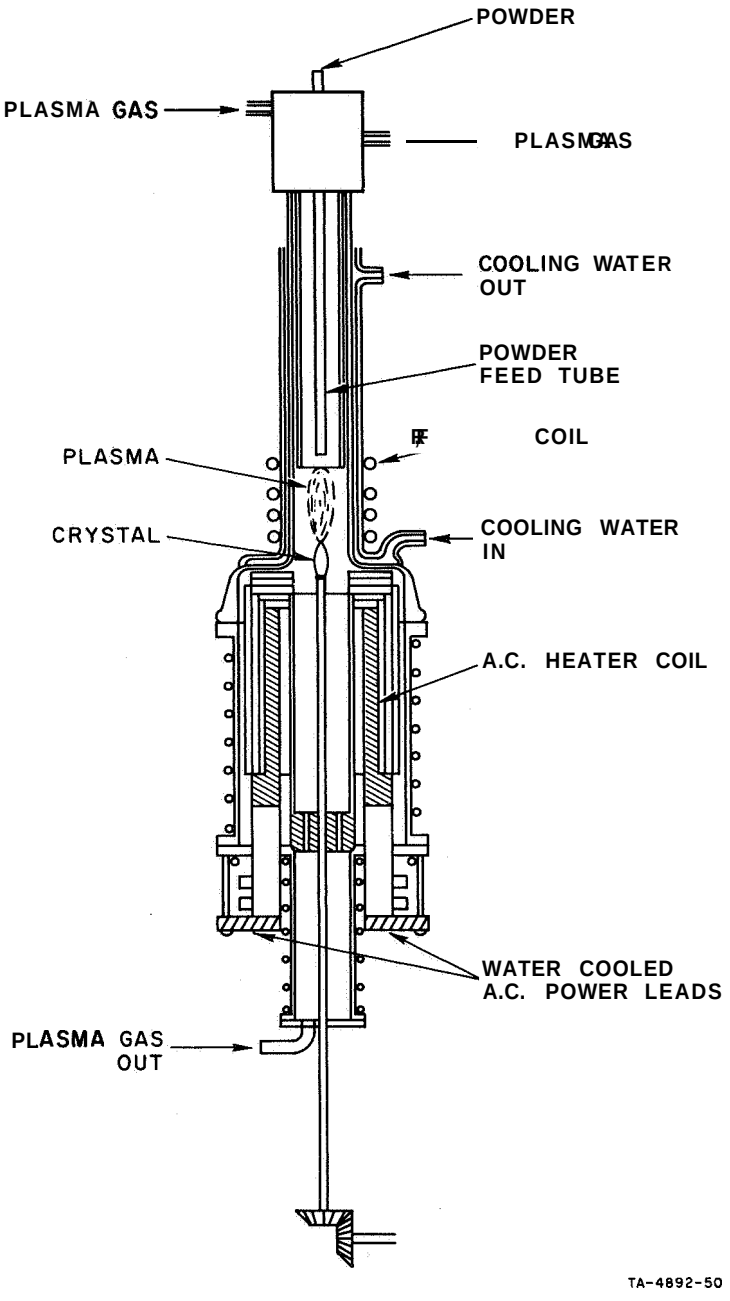

FIG.22 SKETCH OF THE R-F PLASMA VERNEUIL CRYSTAL GROWTH FURNACE

B. Summary of Results

Initial work using the induction-coupled plasma torch as a heat source for Verneuil growth was directed toward forming a stable molten cap on a crystal pedestal. Although the power level was increased through successive experiments, we were unable to melt hafnium carbide or tantalum carbide. Additions of hydrogen to the argon plasma, which were expected to increase the plasma temperature, were not sufficiently effective to permit melting of the carbides or tantalum metal, Optical absorption by the plasma, water, and the quartz containment tube prevented accurate optical pyrometric determinations of seed temperatures, but a disappearing filament pyrometer was used for comparative measurements.

With the carbide seed tip in the hottest part of the plasma, several variations in coil design and oscillator frequency were evaluated to determine whether melting could be obtained. By changing from a five-turn cylindrical coil approximately 3 inches in height to a flat coil, the plasma was shortened considerably but the seed temperature at the hottest point was not changed significantly. Variations in oscillator frequency from 4.8 to 5.6 megaHertz did not affect the temperature as long as the circuit was well tuned.

With these factors optimized, the plasma enthalpy was again increased to see if melting could be obtained. At 21 kw, using a pure argon plasma, incipient melting of a tantalum rod began (mp 2996°C). Tantalum carbide was unaffected at this power level even with hydrogen additions to 20% by volume.

At the 21-kw power level, problems began to arise with the water-cooled quartz plasma containment tube. Although the tube permitted high velocity, vortex coolant flow, water began to boil on the inside surface of the inner tube. More importantly, if the plasma was slightly deflected to one side of the tube, either by a small misalignment of the sheath tube or by tilting the coil, a brown reaction layer formed on the quartz wall. Once this layer formed, heat absorption in the wall increased rapidly and the tube failed catastrophically within a few minutes.

During one run, the power level was increased rapidly to determine at what power level tantalum carbide could be melted. Melting was initiated at the seed tip at 36 kw and 20% hydrogen-80% argon. The power had to be lowered almost immediately, however, so data on melt stability could not be obtained. This behavior should be contrasted with that of aluminum oxide (mp 2050°C), where a large molten cap can be maintained using the same plasma equipment at 10 kw in pure argon and at 3.5 kw with a 50% oxygen addition to the argon. However, radiation losses increase by a factor of five in increasing the melting point from that of aluminum oxide to tantalum carbide.

We had previously found that a vapor-deposited metal film applied to the quartz tube acted as a reflector and assisted in reducing radiation losses and in raising the effective plasma enthalpy at a given power level. Consequently, the plasma containment tube was coated with a thin chromium layer by evaporation to see if this significantly altered the previous findings. This coating was not effective in melting the carbides of interest at power levels that could be maintained over extended periods.

C. Conclusions

At the initiation of this program, it appeared that the induction coupled plasma torch was well-suited for Verneuil growth of refractory crystals because of its similarity in many respects to the flame fusion method that has been well established in commercial Verneuil crystal growth for less refractory materials. Indeed, these advantages continue to appear attractive for many crystals. However, as a result of the difficulties encountered in constructing a practical plasma torch that can operate reliably at very high energy levels, it does not appear that a crystal growth facility useful for the most refractory carbides will be forthcoming with this method. Although induction plasma temperatures can be extremely high, the plasma enthalpy determines the amount of energy transferred to the seed and the ultimate seed temperature. Plasma enthalpies are limited by the low gas pressures that can be attained in stable induction plasmas.

V SOLUTION GROWTH

A. Solvent Restrictions

Solution growth techniques for preparation of carbide crystals require a solvent with the following requirements: adequate solubility of tantalum, hafnium, and carbon; variation of solubility with temperature; sufficiently low melting point; absence of side reactions with crucible materials; low vapor pressure; absence of compound formation between the solvent and the crystal components; and a favorable segregation coefficient with the crystal, i.e., absence of contamination of the crystal by the solvent.

Small tantalum carbide and hafnium carbide crystals can be grown by precipitation in a large number of liquid metals or menstruums. However, because of the high chemical stability of these carbides the concentrations of tantalum, hafnium, and carbon dissolved in the menstruum and in equilibrium with the carbides is very low, regardless of the solubilities of these elements when present separately in the solution. Tantalum and carbon in excess of their equilibrium concentrations will quickly react to form additional tantalum carbide. If this process occurs too rapidly, excessive nucleation and growth of many fine crystals, rather than a few large crystals, will result.

From the thermodynamic viewpoint, two general approaches are available for offsetting the tendency toward excess nucleation in the menstruum. These are: (1) equilibrium or reversible growth based on additions of the carbide compound to the menstruum (rather than the reactive elements), partial dissolution of the carbide, and regrowth of crystals in a thermal gradient; and (2) irreversible carbide precipitation using metal solutions with very low solubilities for tantalum and/or carbon in order to limit the amount of supersaturation (concentration in excess of equilibrium). In the latter case, excess tantalum and excess carbon

are added directly to the menstruum, but precipitation of the carbide occurs very slowly because of the very low concentration of one or both components.

The transition metals, have a high solubility for both tantalum and carbon, and are unsuitable for irreversible growth. However, they offer the best chance of attaning high enough concentrations of carbon and tantalum in equilibrium with tantalum carbide to permit adequate transport rates for crystal growth using the equilibrium or reversible method.

Important thermodynamic and kinetic considerations regarding solution growth of tantalum carbide are discussed in Appendix B. The results of this analysis indicate that the concentrations of components in the most favorable metal solutions for equilibrium growth, 3-d transition metals, will not be sufficient to provide adequate mass transport rates unless both free tantalum and free carbon (usually in the form of a graphite crucible) are eliminated from the system, and tantalum carbide is the only source of either component for crystal growth. With this favorable set of circumstances, the estimated maximum crystal growth rate under conditions of free convective mixing of the menstruum in the crucible is 1 mm/day if a very high growth temperature (1800°C) is maintained and there is a temperature difference between the nutrient and crystal of 100°C. Thus, it appears that equilibrium growth of tantalum carbide in menstruums of the 3-d transition metals is feasible, although marginally so. The results for hafnium carbide are similar.

Liquid metals with low solubilities for both carbon and tantalum (hafnium) were sought for irreversible growth experiments. In some metals the solubilities were so low that crystal growth was precluded (tin). In other solvents slow growth occurred. Aluminum was a good example of a solvent with low solubilities for carbon, permitting slow growth of reasonably large crystallites.

B. Experimental Methods

Two Czochralski crystal growing furnaces designed at Stanford Research Institute were used for all the experiments. These furnaces, one

of which is shown in Fig. 23, employ a graphite resistor heater element of 4 inches ID. The heating elements is surrounded by adequate radiation shields and insulation. The crucible is lowered or raised by a pedestal which travels through O-ring seals in the bottom of the furnace. Seed crystals can be lowered or raised by an upper O-ring housing and the seed crystals can be rotated. Lowering-raising and rotation speeds are variable over several orders of magnitude, typical of a Czochralski crystal growing apparatus. Contaminating gases were removed by evacuation with an oil diffusion pump. The furnace was usually backfilled with helium to retard solvent evaporation. Temperature gradients were controlled by the relative elevation of the crucible within the heater element.

Temperature was automatically monitored and controlled within $0.1^{o}C$ using a Leeds and Northrup radiation pyrometer focused on the bottom of the crucible. The temperature at the meniscus of the melt (upper temperature) was manually monitored using a disappearing filament optical pyrometer.

Three general types of crystal growth experiments were made: (1) growth on the walls or bottom of the crucible resulting from either equilibrium growth using a temperature gradient or continuous introduction of tantalum or carbon to the solution; (2) growth on a seed crystal or probe inserted in the melt; and (3) traveling solvent experiments (TSM), in which a small volume of solvent was used in an attempt to transfer tantalum carbide across a liquid film of metal from one tantalum carbide interface to another. In the TSM experiments, a modified heater element was used to concentrate heat within the liquid metal transfer zone and provide the steepest possible temperature gradient in this region.

C. Summary of Results

Small tantalum carbide crystals were grown using both the irreversible and equilibrium approaches. The crystals appeared as small octahedrons (Fig. 24) or as cubes (Fig. 25). The largest crystals, approximately 0.2 mm, were grown in an aluminum melt using an Al_2O_3 crucible and irreversible growth techniques. Growth on seeds of hot-pressed

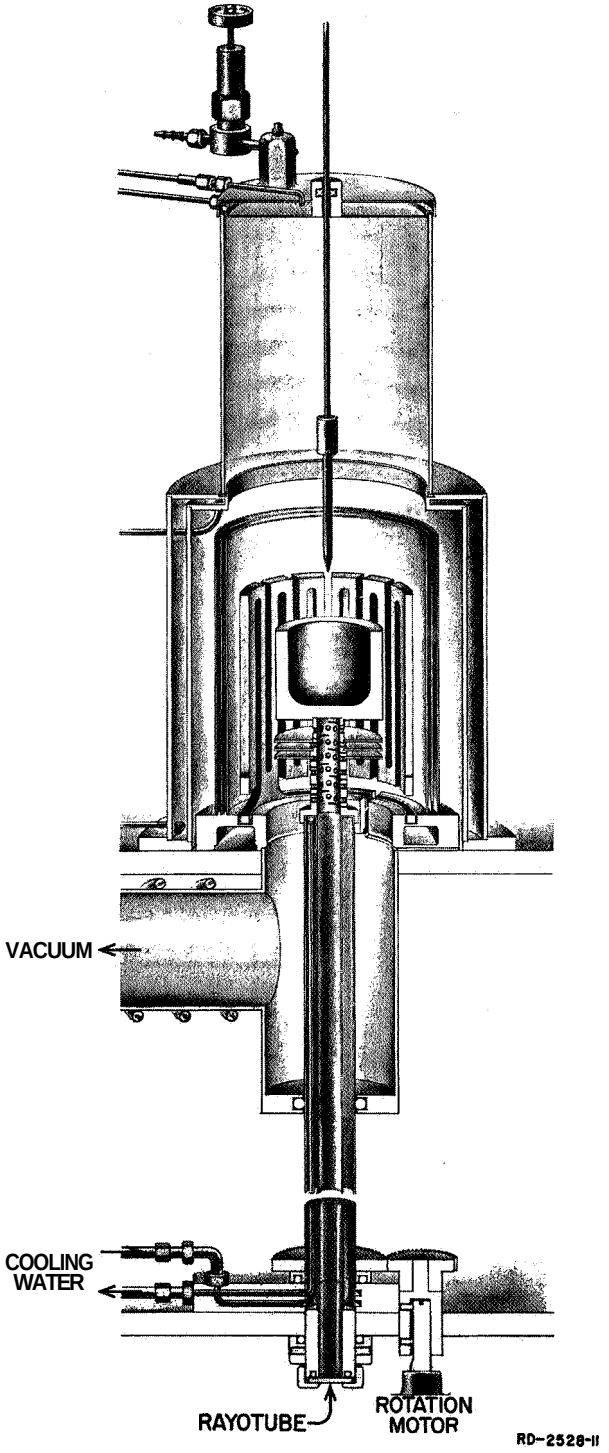

FIG. 23 CZOCHRALSKI CRYSTAL GROWING FURNACE USED IN SOLUTION GROWTH EXPERIMENTS

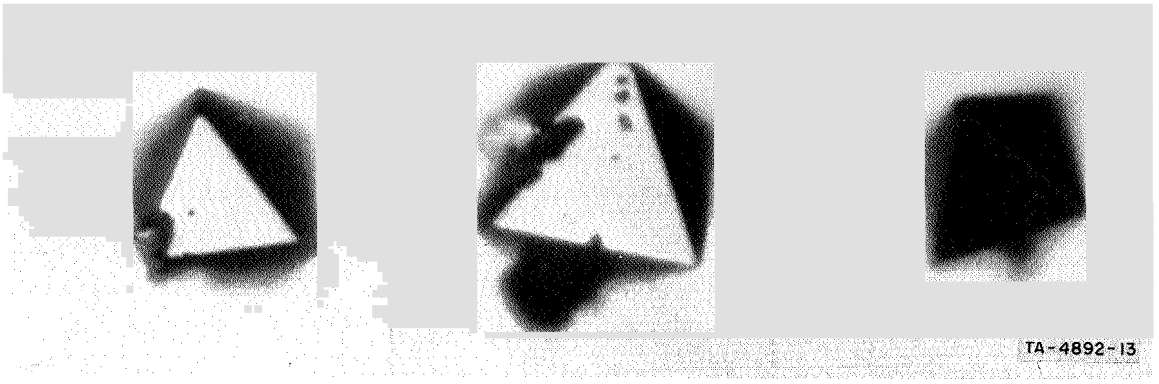

FIG. 24 TANTALUM CARBIDE CRYSTALS GROWN USING ALUMINUM SOLVENT (400X)

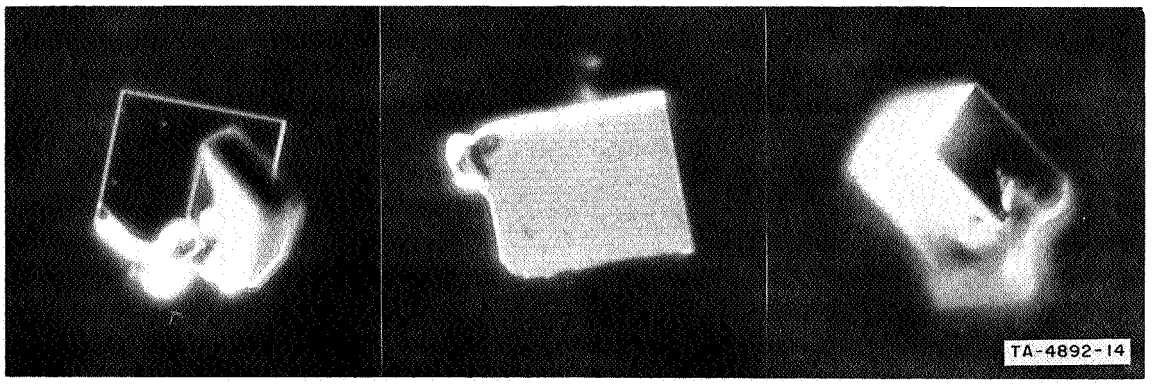

FIG. 25 TANTALUM CARBIDE CRYSTALS GROWN USING AN IRON–TIN ALLOY SOLVENT (400X)

tantalum carbide, and tantalum carbide boules, and on probes of graphite, tantalum, or aluminum oxide inserted into the solutions was not successful.

Spontaneous nucleation and continuous distribution of fine tantalum carbide crystals throughout the solution was the major factor preventing growth on seed crystals. This distribution of fine tantalum carbide crystals throughout the solution was verified by sampling menstruums during growth experiments. Spectrographic analysis of these samples indicated that the tantalum concentration was much higher than the tantalum carbide equilibrium concentration would permit. Further tests of menstruums with larger additions of tantalum (12 at. $) using X-ray fluorescence analysis indicated higher apparent tantalum contents in the solutions. In all cases the measured tantalum fraction was nearly equal to the tantalum fraction initially placed in the crucible. The results are summarized in Tables V and VI.

Table V

TANTALUM CONTENT BY SEMIQUANTITATIVE EMISSION SPECTROGRAPHIC ANALYSIS OF CARBON-SATURATED LIQUID METALS IN CONTACT WITH TANTALUM CARBIDE

Run No.	Initial TaC Addition (wt %)	Liquid Metal	Equilibration Period (hours)	Ta Content of Sample (wt %)
38	1.5	Iron	1	2.0
			1	1.5
			6	2.5
			24	2.5
39	1.5	Nickel	1	1.25
			1	2.0
			6	2.5
			24	2.5
43	1.5	Aluminum	1	nil

Table VI

TANTALUM CONTENT BY X-RAY FLUORESCENT SPECTROGRAPHIC ANALYSIS OF CARBON-SATURATED LIQUID METALS IN EQUILIBRIUM WITH TANTALUM CARBIDE

Run No.	Initial Ta Addition (wt %)	Liquid Metal	Equilibrium Period (hours)	Ta Content of Sample (wt %)
46	13.8	Iron	1	12.2
			6	12.5
			24	12.5
47-2	15	Nickel	1	15.3
			3	13.5
			6	21.1
			24	12.8

X-ray diffraction analyses after quenching samples proved that the excess tantalum was in the form of tantalum carbide rather than dissolved tantalum. These tests, which were done on a number of samples taken at various times in different solutions, proved the occurrence of a continuous distribution of fine tantalum carbide in the solution. This condition prevented an effective concentration gradient and supersaturated region in the solution surrounding the seed, which are required for growth to occur. Baffling to retard convective mixing of the menstruum was considered to be impractical.

Hot-pressed tantalum carbide bodies tended to disintegrate at grain boundaries in metal solutions and provide particles for dispersion. Tantalum carbide melted boules, which became available later in the program as a result of the melt-growth experiments, dissolved uniformly but nucleation and dispersion of fine tantalum carbide crystals in the solution was still sufficient to prevent crystal growth on seeds.

Platinum and iron were used as solvents in TSM experiments. Platinum was used because it has a higher specific gravity than tantalum carbide, a condition with some experimental advantages. Platinum possesses appreciable solubility for tantalum and some solubility for carbon. Two tantalum carbide sections were separated by the liquid metal solvent

within a crucible and subjected to a steep temperature gradient. These experiments did not produce significant transport of tantalum carbide from one interface to the other interface in either iron or platinum, probably because of inadequate solubility of the diffusing components.

Stockbarger experiments using an iron solution in a tapered boron nitride crucible failed to produce large single crystals of tantalum carbide.

D. Conclusions

Because of the low solubility of tantalum and carbon in equilibrium with tantalum carbide in liquid metal solutions and the inability to control spontaneous nucleation of tantalum carbide crystals, growth of large single crystals suitable for physical properties measurement by the solution growth technique was not found to be feasible.

VI ANALYTICAL PROCEDURES AND RESULTS

All the carbide powders used in crystal growth experiments were secured from Wah Chang Corporation, Albany, Oregon. Typical spectrographic analyses of carbide starting materials are shown in Table VII. Results are given for TaC, HfC, 40% HfC/60% TaC, and 20% HfC/80% TaC. Because of the high zirconium content of the hafnium carbide, some crystal growth experiments were conducted using a spectrographic grade of hafnium carbide which was free of zirconium. However, this did not produce any change in crystal growth behavior.

A. Impurity Analysis

In Table VIII a spectrographic analysis of impurities in a typical tantalum carbide boule is compared with the analysis of the starting powder used to grow the boule. Although these analyses were conducted by different laboratories, the agreement is quite good. There is no evidence of an increase in impurity content, with the possible exception of tungsten, nickel, and titanium, and these differences appear to be within experimental error.

B. Carbon Content by Lattice Parameter Measurement

The use of precise lattice parameter measurements to determine carbon stoichiometry has been mentioned. The experimental procedure was to grind a section of each boule, usually the upper portion, in a small mortar. The resulting powder sample was examined by X-ray diffraction in the back reflection region using a back reflection focusing camera or a Debye-Scherer camera. Lattice parameters were determined to four significant figures using standard film reading and data reduction procedures. This was done for every worthwhile tantalum carbide boule. Lattice parameters varied between 4.418 Å and 4.435 Å ($TaC_{0.86}$ and $TaC_{0.92}$, respectively). For a great many of the boules the lattice parameter was very close to 4.430 Å ($TaC_{0.90}$).

Table VII

ANALYSIS OF CURRENT CARBIDE STARTING MATERIALS (ppm)
1 November 1966

Impurity	TaC	HfC	40% HfC 60% TaC	20% HfC 80% TaC
Al	<10	< 25	500	20
B	< 1	5	10	5
Cb(Nb)	<50	<100	490	--
Cd	< 1	< 1	< 1	< 5
co	< 5	--	< 5	<10
Cr	15	175	<10	<20
cu	<10	< 40	15	<40
Fe	70	520	380	150
Mg	<10	< 10	<10	<20
Mn	<10	< 10	<10	<20
Mo	<10	10	10	<20
Ni	<10	10	40	<20
O	179	2720	3400	790
Pb	< 5	< 5	< 5	<20
Si	30	< 40	30	<40
Sn	<10	< 10	<10	<20
Ta	--	<200	--	--
Ti	<lo	175	<lo	<50
V	<10	< 5	<10	<20
W	--	< 20	--	--
Zn	<lo	--	<lo	<50
N	132	--	55	35
C,wt.%	6.16	5.97	6.28	6.06
C,at.%*	49.5	47.5	50	48.6
Zr	<50	3.15 wt.%	--	--

* Apparent atom percent since free carbon is included.

Material		Wah Chang Lot No.
Tantalum carbide		SP106526B
Hafnium carbide		SP8662A
40% hafnium carbide	60% tantalum carbide	SP86617A
20% hafnium carbide	80% tantalum carbide	SP86615B

Table VIII

ANALYSIS OF TANTALUM CARBIDE STARTING POWDER AND ARC-VERNEUIL BOULE

Impurity	Powder* (ppm)	Boule (3/9/67)† (ppm)
Al	< 10	20
B	< 1	nil
Cb (Nb)	< 50	200
Cd	< 1	nil
Co	< 5	10
Cr	15	10
Cu	< 10	10
Fe	70	80
Mg	< 10	20
Mn	< 10	40
Mo	< 10	20
Ni	< 10	70
O	179	Not reported
Pb	< 5	< 10
Si	30	60
Sn	< 10	20
Ti	< 10	300
V	< 10	10
W	Not reported	100
Zn	< 10	< 50
N	132	Not reported
Zr	< 50	< 50

* Wah Chang Analysis of Lot SP106526B.

† Analysis by Metallurgical Laboratories, Inc., San Francisco.

C. Impurity Analysis at Grain Boundaries (Microprobe)

A typical tantalum carbide boule containing grain boundaries was examined by electron microprobe analysis at Materials Analysis Company, Palo Alto, California. The crystal specimen was mounted and polished at the Institute, and selected spots on grain boundaries, subgrain boundaries, and at grain boundary nodes were marked with microhardness indentations. The procedure was to place two microhardness indentations on either side of the grain boundary or subgrain boundary, and to mark grain boundary nodes with three indentation marks equally spaced about the node center. Before microprobe analysis, the specimen surface was lightly polished to remove the etch relief without obscuring the indentation marks. Location of the microprobe electron beam on the preselected spot was facilitated by the indentation marks. The correct location of the mircroprobe analysis was subsequently confirmed by metallographic examination of the spot formed on the specimen by the electron beam.

Grain boundaries were microprobed at four different spots and an electron beam spot size of from 1 to 1-1/2 μ diameter was used in each analysis. All elements of Atomic No, 14 (Si) and higher were included in the spectro-scans made at each spot. Except for tantalum, no elements were detected in the analyses. The limits of detection for some of the potential grain boundary impurity elements are given in Table IX. These limits of detection are given in terms of the small region stimulated by the beam rather. than the entire specimen.

Table IX

LIMITS OF DETECTION ON MICROPROBE ANALYSIS OF $TaC_{0.9}$

Element	Limit of Detection (wt %)
Si	0.1
Fe	0.1
Ti	0.1
Mg	0.2
Ni	0.2
Zn	0.2

The results indicate that all the impurity elements above Atomic No. 14 are dissolved in the crystal and do not segregate at grain boundaries. Thus, impurity segregation was ruled out as a probable cause of the nucleation of new grains.

D. Metallographic Specimen Preparation

Metallographic polishing procedures for the carbide boules consisted of the following: (1) hand grinding on 600-grit silicon carbide paper, (2) polishing with a 6-micron diamond on a Politex Pre-P.S. cloth (Geoscience Instrument Corp.), and (3) polishing with 0.25 μ diamond using an automatic vibratory Syntron lap and the Politex Pre-P.S. cloth. Although other etchants were occasionally used, superior results were obtained with the following procedures. Tantalum carbide boules were immersed in three parts HNO_3 and one part HF. Hafnium carbide boules were immersed in three parts HCl, one part HNO_3, and one part HF, which left the surface stained. The sample was then swabbed with one part H_2O and one part NH_4OH to remove the stain.

E. Orientation of Crystals

Boules were oriented for crystal cutting using back-reflection Laue photographs. Each boule was cross sectioned near its cap and attached to a single crystal goniometer with hard wax. The first Laue photograph was taken with the boule axis parallel with the X-ray beam. Because a [100] direction is usually within 20° of the boule axis, the required rotations of the crystal to bring the (100) face perpendicular to the X-ray beam could usually be estimated from the first Laue photograph and a 100 stereogram. Final alignment of the (100) face within 2° often required a second and third correction in the alignment, each followed by a Laue photograph. Once the (100) face was aligned, the goniometer was removed from the X-ray machine and mounted on a diamond cut-off machine. A cut parallel with the (100) face was taken while the crystal remained mounted to the goniometer and without further adjustment. Orientation of the cut face was verified by another Laue photograph taken with the cut face normal to the X-ray beam. Further cuts were taken using the (100) diffraction pattern to indicate the orientation of perpendicular

{110} and {100} planes, i.e., planes oriented 90° from the (100) face. A large number of Laue photographs were required in processing boules. A molybdenum X-ray tube and Polaroid film were used to reduce the exposure time for each photograph to one minute.

Laue photographs were also used to confirm that the boules were single crystals. This was done by comparing several Laue photographs taken at different locations on the crystal.

Laue photographs also gave information on the extent of misorientation of subgrains within a given crystal. As an example, the two Laue photographs shown in Fig. 26 were taken from different areas of the same (100) face of a tantalum carbide crystal. While there is little misorientation in the upper photograph, the lower photograph shows a smear of points for each diffracting plane caused by diffraction from several subgrains, each with a slightly different orientation. The total misorientation spread in this region was approximately 3°. The misorientation of subgrains shown in Fig. 26 also appears to have a systematic trend with all the points on a straight line. This situation was fairly common and in the case shown it can be explained by rotation about a <110> axis. Similar simple orientation relationships between grains within boules were also observed.

Several single crystal bars of $TaC_{0.9}$ with all faces cut parallel to {100} are shown, before polishing, in Fig. 27.

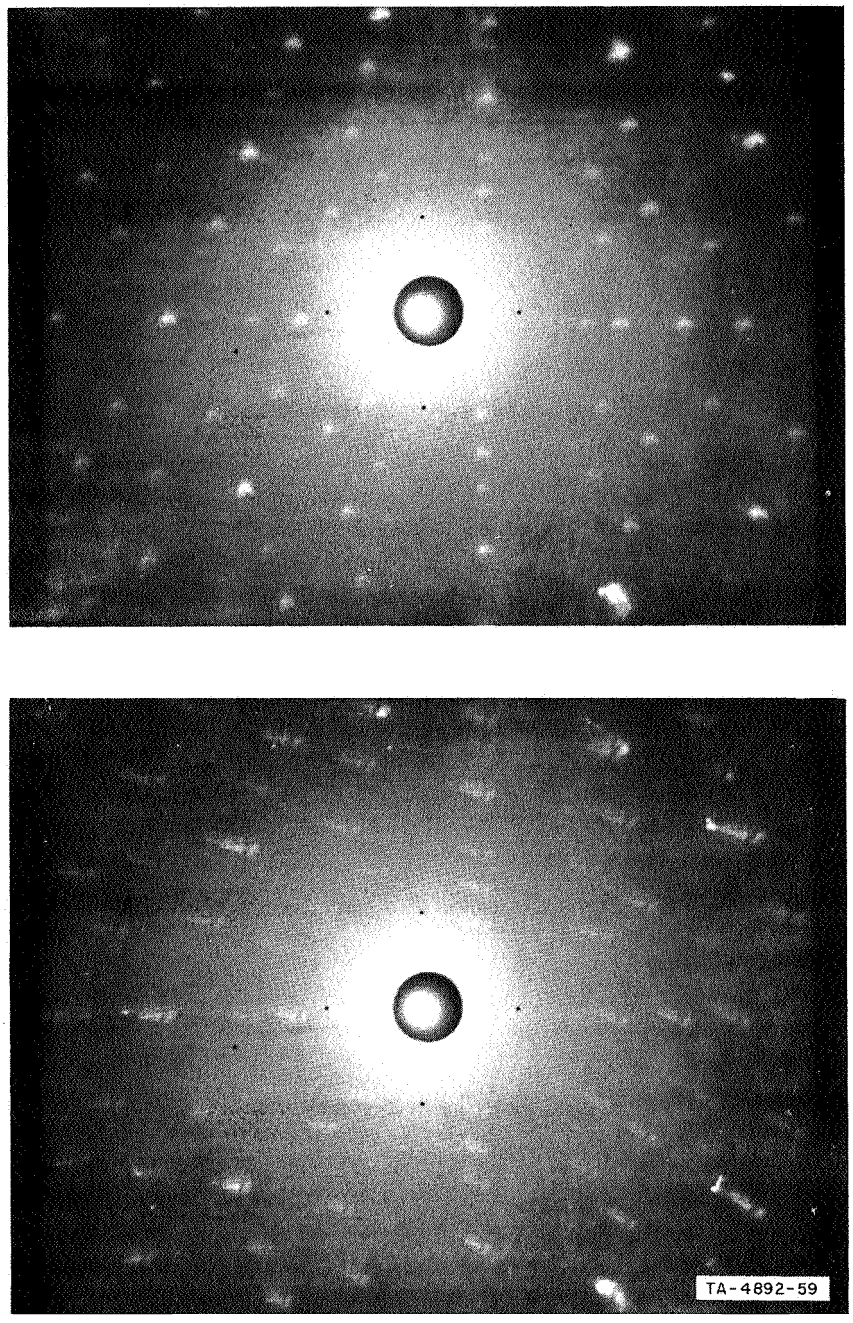

FIG. 26 TWO LAUE PHOTOGRAPHS OF A (100) SURFACE OF $TaC_{0.9}$ SHOWING INCREASED MISORIENTATION OF SUBGRAINS IN THE LOWER PHOTOGRAPH

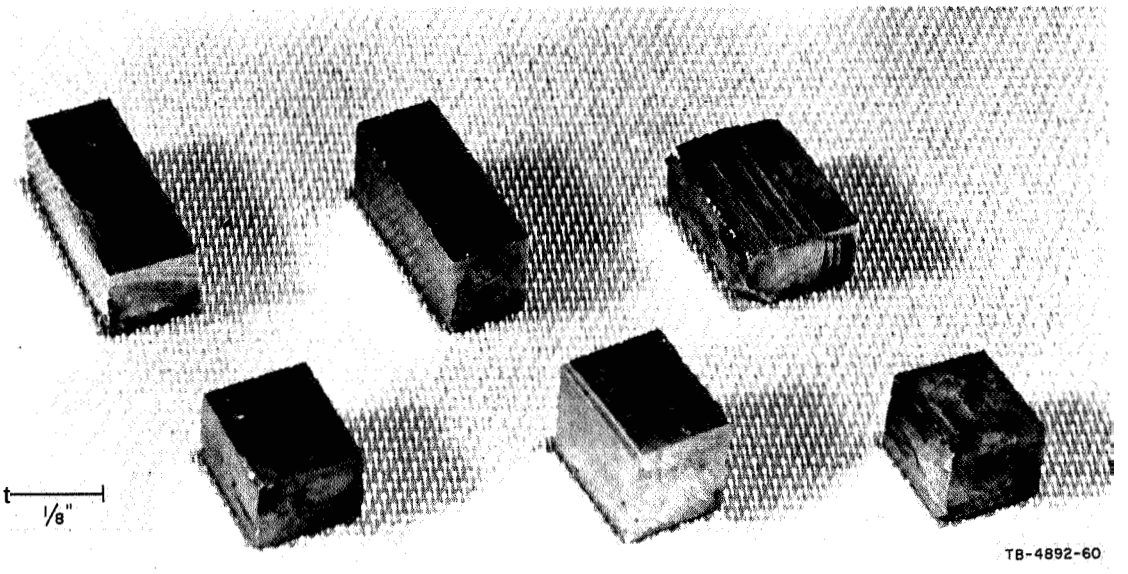

FIG. 27 $TaC_{0.9}$ CRYSTALS WITH ALL FACES CUT PARALLEL TO {100}

VII ELASTIC CONSTANTS OF $TaC_{0.90}$

Because of their high degree of symmetry, cubic crystals have only three independent elastic constants[12]: C_{11}, C_{12}, and C_{44}, corresponding with dilation normal to the stress, perpendicular to the stress, and in shear. These elastic constants were determined for $TaC_{0.90}$ by measuring the velocity of an ultrasonic pulse generated by a quartz transducer and transmitted through the test crystal. In the pulse-echo technique, the sound is reflected from the rear surface of the crystal back to the transducer. In the double transducer technique, one transducer is used to initiate the pulse while the other is used as a detector attached to the rear surface. Both methods were used with $TaC_{0.90}$ crystals with equal success. Longitudinal velocities were determined with better reproducibility than were the transverse velocities.

Velocities were measured in the $<100>$ and $<110>$ directions using two single crystals cut from the same $TaC_{0.90}$ boule. The density of these crystals calculated from their composition and lattice parameter is 14.65 g cm^{-3}. Both crystals were carefully cut and polished so that their front and back faces were parallel within 0.3% of their separation distance and normal to the $<100>$ and $<110>$ directions, respectively, within 1°, as determined by Laue photographs. The transducers were attached with Nonaq stopcock grease.

The longitudinal velocity V_L and the two transverse (shear) velocities, V_T and V_t are related to the elastic constants C_{ij} and density ρ according to the following relations:[13]

for $<100>$: $\rho V_L^2 = C_{11}$

$\rho V_T^2 = \rho V_t^2 = C_{44}$

for $\langle 110 \rangle$: $\rho V_L^2 = (C_{11} + C_{12})/2 + C_{44}$

$$\rho V_T^2 = (C_{11} - C_{12})/2$$

$$\rho V_t^2 = C_{44} \quad .$$

The measured velocities for $TaC_{0.90}$ were as follows:

$\langle 100 \rangle$ $V_L = 5.88 \pm 0.07$ km/sec

$\langle 100 \rangle$ and $\langle 110 \rangle$ $V_t = 2.32 \pm 0.10$ km/sec

$\langle 110 \rangle$ $V_L = 5.02 \pm 0.07$ km/sec

$\langle 110 \rangle$ $V_T = 3.76$ km/sec (1 reading) .

The calculated elastic constants are compared in Table X with data[14] on TiC, also obtained with an ultrasonic pulse technique.

Table X

ELASTIC CONSTANTS OF $TaC_{0.90}$
(10^{12} dynes cm^{-2})

Elastic Constant	$TaC_{0.90}$	TiC[14]
C_{11}	5.05 (± 2%)	5.00
C_{44}	0.79 (± 8%)	1.75
C_{12}	0.73*	1.13
	0.91† (+25%) (Est.)	

* From: $\rho V_L^2 \langle 110 \rangle = (C_{11} + C_{12})/2 + C_{44}$.

† From: $\rho V_T^2 \langle 110 \rangle = (C_{11} - C_{12})/2$.

VIII RECOMMENDED ADDITIONAL WORK ON PHYSICAL PROPERTIES

Because of the interest in high temperature aerospace applications of tantalum carbide, a study of plastic deformation in $TaC_{0.9}$ crystals generated under the present program is recommended. This program should include a study of the stress-strain relationships, determination of the critical resolved shear stress dependence on temperature and strain rate, and determination of slip systems. Hot compression loading[15] is suggested as the experimental technique best suited to the available crystals. By correlating hot compression testing with hot microhardness testing on single crystals of $TaC_{0.9}$, it may be possible to estimate the behavior of tantalum monocarbide single crystals containing higher carbon concentrations from hot microhardness tests performed on polycrystalline tantalum carbide.

Effort should also be directed to the development of diffusional procedures, at temperatures greater than 2500°C, for altering the carbide crystal stoichiometry within the single phase composition range. The use of hot hardness testing as a tool in such investigations, as well as hot compressive testing, should provide a considerable advance in understanding of carbide behavior.

APPENDIX A

VAPORIZATION AND STOICHIOMETRY IN REFRACTORY CARBIDES - A LITERATURE REVIEW

A considerable amount of literature data has accumulated on vaporization rates, composition of vapors, and changes in composition for various carbides at elevated temperatures. In the course of this program this information was evaluated and applied to the growing of single crystals of hafnium carbide, tantalum carbide, and their solid solutions.

I. Tantalum Carbide

A. Vapor Pressure

The values for total vapor pressure of tantalum carbide, essentially carbon, as calculated from vaporization data by Hoch[16] and Coffman[17], are in agreement, and are shown as a single line in Fig. 28; however, the results have the inherent experimental disadvantage that the vapor pressure decreases with decrease in carbon concentration, and the results at the higher temperatures are for a lower average carbon ratio than are those obtained at the lower temperatures. The lines calculated by Kaufman[18] at 46 and at 50 at. % carbon have a steeper slope than the experimental data.[16,17] The curves have been extrapolated to temperatures around 3700°C (3973°K).

The effect of sample composition on the vapor pressure can be seen more easily in Fig. 29, which gives the vapor pressures of tantalum and carbon at 2730°C (3000°K) and 4000°C (4273°K). This should be compared with the phase diagram in Fig. 1. The vapor pressure data at 2730°C for the solid are taken from Kaufman[18] for the range of 41 to 50 at. % carbon. The other vapor pressure curves are estimated from the extrapolated data of Fig. 28 and should be considered as schematic rather

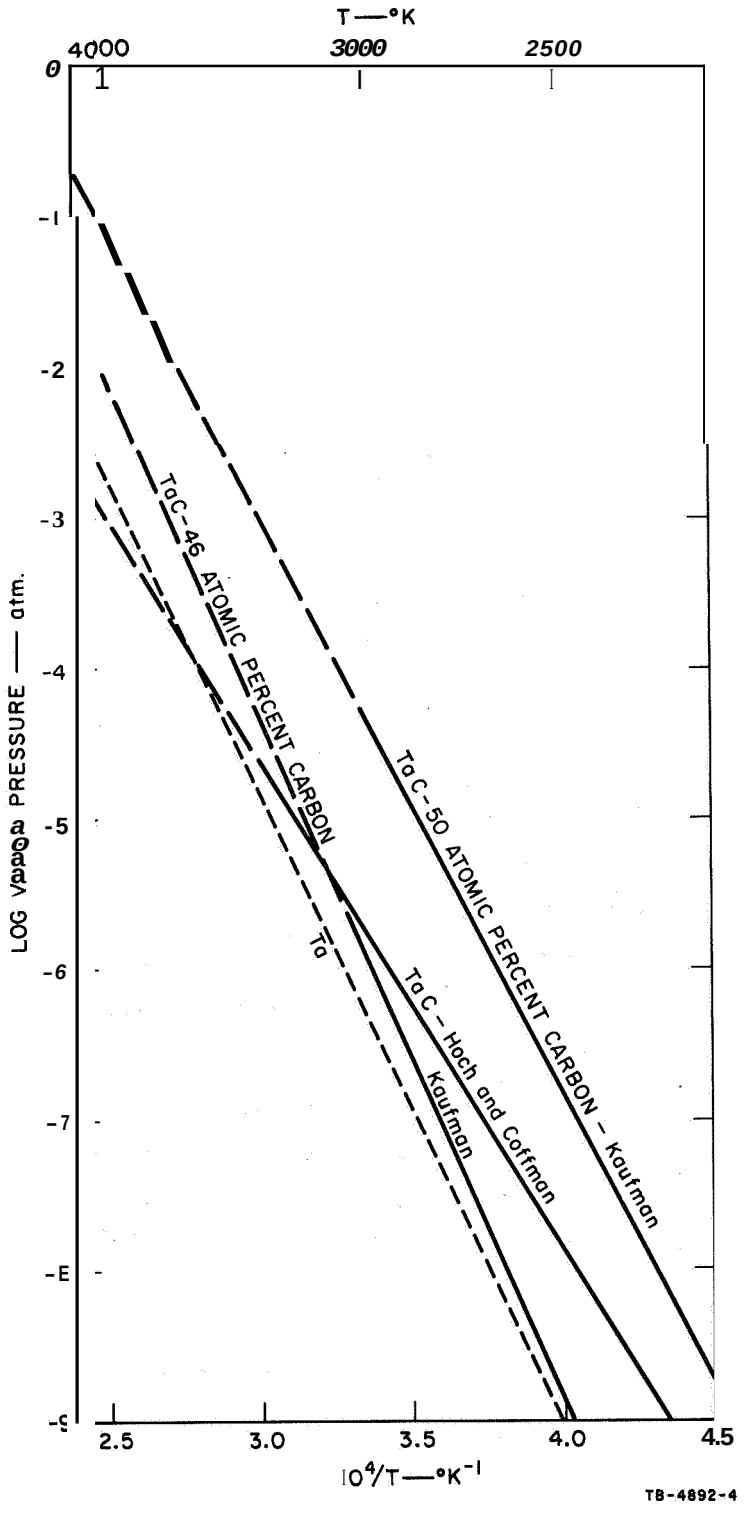

FIG. 28 VAPOR PRESSURE OF TANTALUM CARBIDE

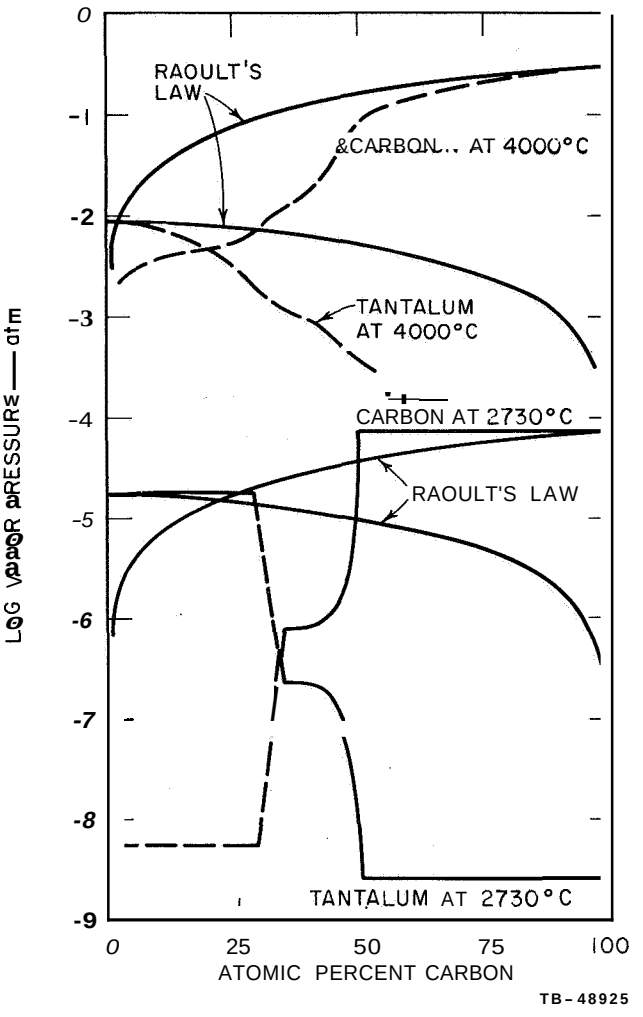

FIG. 29 VAPOR PRESSURES OF To-C SYSTEM

than as having the correct magnitude. The vapor pressure curves that would apply if Raoult's law were obeyed are shown, and the curves for the liquid at 4000°C are shown as deviating less than the vapor pressure curves for the solid at 2730°C.

B. Vaporization Rate

1. Previous Studies

Most of the vaporization studies reported in the literature to date have been performed in vacuum and all have been below the temperature of the TaC–C eutectic, which occurs at about 3300°C. Studies in vacuum by Hoch[16] from 1960°C (2233°K) to 2490°C (2763°K) and Coffman[17]

from 2360°C (2633°K) to 3110°C (3383°K) agree.** The data by Hoch and Coffman at the higher temperatures are for a lower average carbon ratio than those at the lower temperatures. Kaufman[18] has calculated the vaporization rates, and his data are shown in Fig. 30 for tantalum carbide containing 46 and 50 at. % carbon. These data require a considerable extrapolation to reach the melting point of about 3800°C (4073°K). The most recent experimental data are those by Deadmore.[8] Note that all of the data in Fig. 30 are for the total vaporization rate and do not distinguish differences in vaporization rates of carbon and tantalum from tantalum carbide.

In a second report on vaporization rates in refractory carbides,[8] Deadmore experimentally confirmed that carbon vaporizes much more rapidly than tantalum from tantalum carbide. At the highest temperature studied, 2600°C (2873°K), the vaporization rate of carbon was nine times the vaporization rate of tantalum. This leads to depletion of carbon and a gradual reduction in the total evaporation rate (sum of both components).

Vaporization into an inert atmosphere was studied by Kempter and Nadler[20] from 1890°C (2163°K) to 3320°C (3593°K). However, they published only the decrease in the molar ratio of C/Ta and did not publish weight loss. Assuming that the loss of tantalum was negligible relative to carbon, we can calculate vaporization rates. (Fries** discusses Kempter's data on niobium carbide and gives the losses in weight percent; these results are from 1.1 to 2.0 times the values that we calculate from the decrease in carbon.) The vaporization rates calculated from Kempter's data at 2715°C (2988°K) to 3320°C (3593°K) are plotted in Fig. 30, but these should be considered as approximate values. The vaporization rate in an inert atmosphere should roughly parallel that in vacuum in the temperature range up to about 3200°C. Also both rates should have a gradually decreasing slope as the temperature approaches the boiling point, owing to a decrease in the rate of diffusion and in the effect of the vaporization products, acting as a diffusion barrier. The vaporization rate in vacuum would have a greater decrease than that in an inert atmosphere.

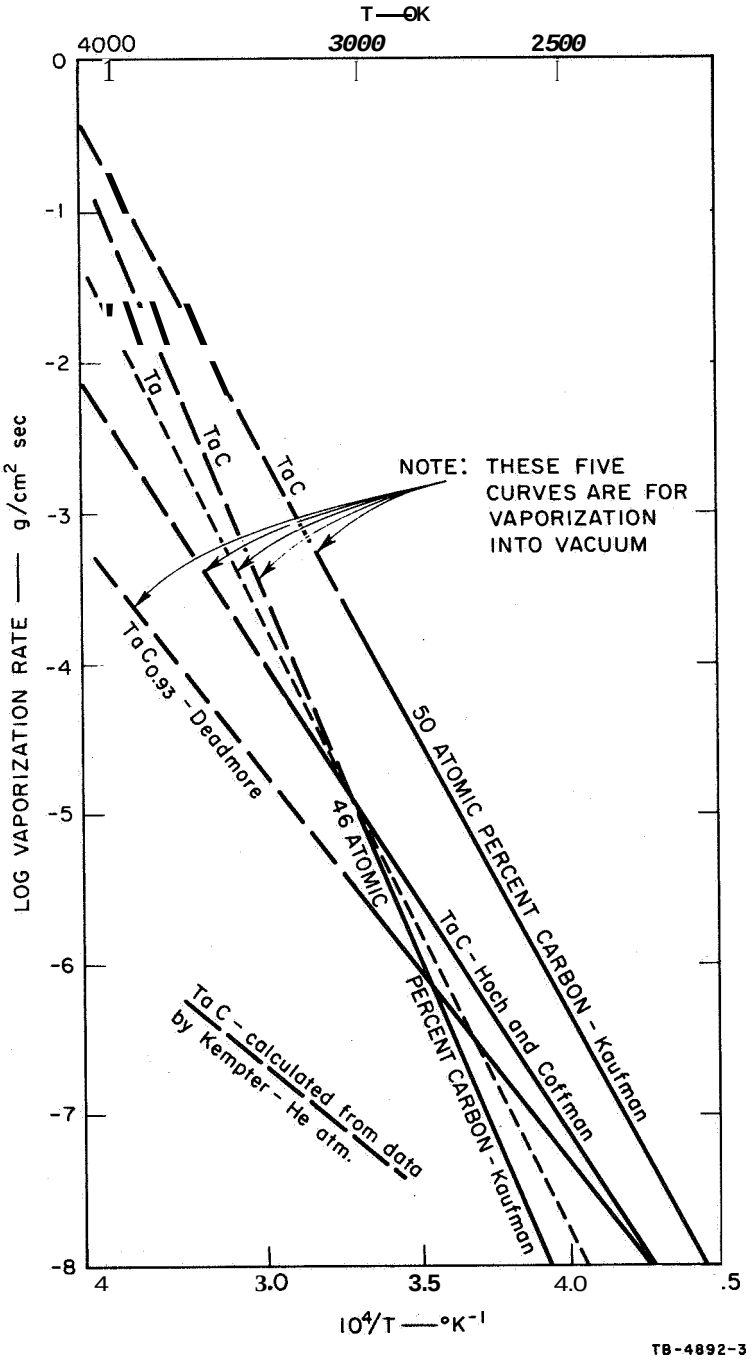

FIG. 30 TOTAL VAPORIZATION RATE FOR TANTALUM CARBIDE

2. Effect of Specimen Shape, Gas Composition, and Pressure

In addition to temperature and sample composition, other factors that influence the vaporization rate include the diameter or shape of the sample, the composition of the inert gas, and the pressure of the inert gas. These factors have been studied by Jones et al.[22] and by Fonda[23,24] for tungsten filaments. In general, they consider that volatilization occurs by diffusion of the gaseous molecules through a stagnant film in which the equilibrium composition is present at the solid-gas interface, and the concentration of the volatilizing species may be negligible at the outer boundary of the film. If volatilization occurs from a filament, the rate increases with decrease in diameter owing to a decrease in the film thickness or to a lower probability that a given atom entering the gaseous film will return to the solid (or liquid) surface.

The equation relating the filament diameter to vaporization rate is

$$m = \frac{\text{constant}}{a \ \ln b/a}$$

where m = vaporization rate, a = filament diameter, and b = gas film diameter. The value of b is calculated from the equation $\ln b/a = 2B/b$, where B is the film thickness over a plane surface (a value of 0.43 cm was used).[23] From this, the evaporation of a 0.2-cm-diameter wire is 2.1 times that of a 1-cm-diameter wire, while the 1-cm wire has an evaporation rate close to that of a flat surface. The vaporization from a tip of a rod would be affected similarly. Since the boules in carbide melt growth were at least 0.5 cm diameter, this factor did not have a significant effect on vaporization. Close spacing of the blunted carbon electrodes further retarded the net vaporization rate.

The choice of inert gas has an effect on the diffusion coefficient which affects the vaporization rate. The equation by Wilke and Lee[25] was used to estimate diffusion coefficients. A knowledge of the molecular volume of the liquid at the normal boiling point is required but is not known for tantalum. Arbitrary values of 50 and 100 cc/g-mole were used for the molal volume of tantalum and gave little difference in

the calculated values of the diffusion coefficient. The calculated diffusion coefficients of mixtures of carbon in hydrogen or argon and of tantalum in hydrogen and argon are given in Table XI. In the case of carbon, the predominant equilibrium species is triatomic carbon, but monatomic carbon is probably volatilized from the surface of the solid or liquid. Assuming that the diffusion coefficient for monatomic carbon applies, the use of argon would give a diffusion coefficient of 0.36 of that in hydrogen, and presumably the volatilization would also be about one-third as much. Also, carbon has a singificantly higher diffusion coefficient than tantalum and would have a higher volatilization even if the decomposition pressures were equal.

Table XI

DIFFUSION COEFFICIENTS AT 3000°K

	V_o (cc/g-mole)	D in H_2 (cm^2/sec)	D in Ar (cm2/sec)	$\frac{D \text{ in } H_2}{D \text{ in Ar}}$
Carbon	14.8	30.6	11.0	2.8
Triatomic carbon	44.4	19.7	5.4	3.6
Tantalum	50	16.7	4.2	4.0
Tantalum	100	14.4	3.2	4.5

The effect of pressure of the inert gas on vaporization has also been studied by Fonda[24] and the vaporization decreased directly with the pressure for pressures greater than 0.15 atm.

C. Application to Melt Growth

So far, the vaporization of tantalum carbide has been discussed in terms of the effect of temperature in vacuum, the vapor pressure of tantalum and carbon in a sample, the effect of sample diameter, choice of inert gas, and pressure of inert gas. However, most of the data apply below 3000°K, and an estimate is still needed of the change in composi-

tion of the sample from the volatilization at the melting point. It seems best to use an arbitrary factor to relate vapor pressure to vaporization rate, even though this may be an order of magnitude in error. Based on Fig. 30, the vaporization rate in helium is a factor of 100 to 1000 less than that in vacuum, or about a factor of 10 to 200 less than the numerical value of the vapor pressure in atmospheres. The data by Fonda showed the calculated vaporization rate of a tungsten 0.2-cm-diameter filament to be a factor of about 1000 less than the numerical value of the vapor pressure in atmospheres. For the rough calculation of change in composition, we shall assume that the vaporization rate in g/cm^2 sec is 0.01 of the numerical value of the vapor pressure in atmospheres. From Fig. 29, the estimated vapor pressure of carbon over liquid tantalum carbide is about 0.04 atm. at 46 at. % carbon and 0.08 atm. at 50 at, % carbon. This gives a carbon vaporization rate of 0.002 $mole/cm^2/min$ over liquid tantalum carbide at 46 at. % carbon and 0.004 $mole/cm^2/min$ at 50 at. % carbon. These rates of loss of carbon might well be an order of magnitude too high owing to the assumptions that were made. In addition, changes of the inert gas compositions may alter these rates by another order of magnitude..

The addition of acetylene was expected to reduce the volatilization of carbon markedly. A mixture of 10% acetylene and 90% argon would produce an equilibrium pressure of carbon of about 0.022 atm. The vapor pressure of carbon over tantalum carbide containing 46 at. % carbon at $4000^{\circ}C$ is 0.04 atm. A sample with about 43 at. % carbon is estimated to be in equilibrium with 10% acetylene.

The results of these calculations indicated that the growth of single phase carbide crystals from the melt was probably feasible. The numbers obtained were very approximate but were certainly close enough to desired equilibrium values to force the issue to be resolved experimentally. It appeared that one would be able to maintain the carbide within the single phase homogeneity range, and maintain specific compositions within this range by proper control of the gaseous environment and the composition of feed powders.

II. Vaporization and Stoichiometry in Melt Growth of Hafnium Carbide

The vaporization of hafnium carbide shows distinct differences from that of tantalum carbide. Figure 31 gives the vapor pressure and vaporization rate data by Coffman[26] and the vaporization rate data by Deadmore[7] along with the calculated data by Kaufman.[16] The experimental data by Coffman showed that hafnium is the predominant vapor over HfC, while carbon is lost from TaC. However, Deadmore, in his second report,[8] shows that hafnium and carbon evaporate at equal rates from HfC. Both Deadmore and Coffman indicate that the total vaporization rate of hafnium carbide at its melting point should be greater than the vaporization rate of tantalum carbide at its melting point. Deadmore shows a greater difference in vaporization rates of these compounds.

The effect of composition (stoichiometry) on evaporation in hafnium carbide systems, calculated by Kaufman, is shown in Fig. 32, which indicates that HfC with 49.8 at. % carbon at 3000°K would be stable (compositionally invariant) during volatilization in vacuum. These calculations are supported by Deadmore's findings.

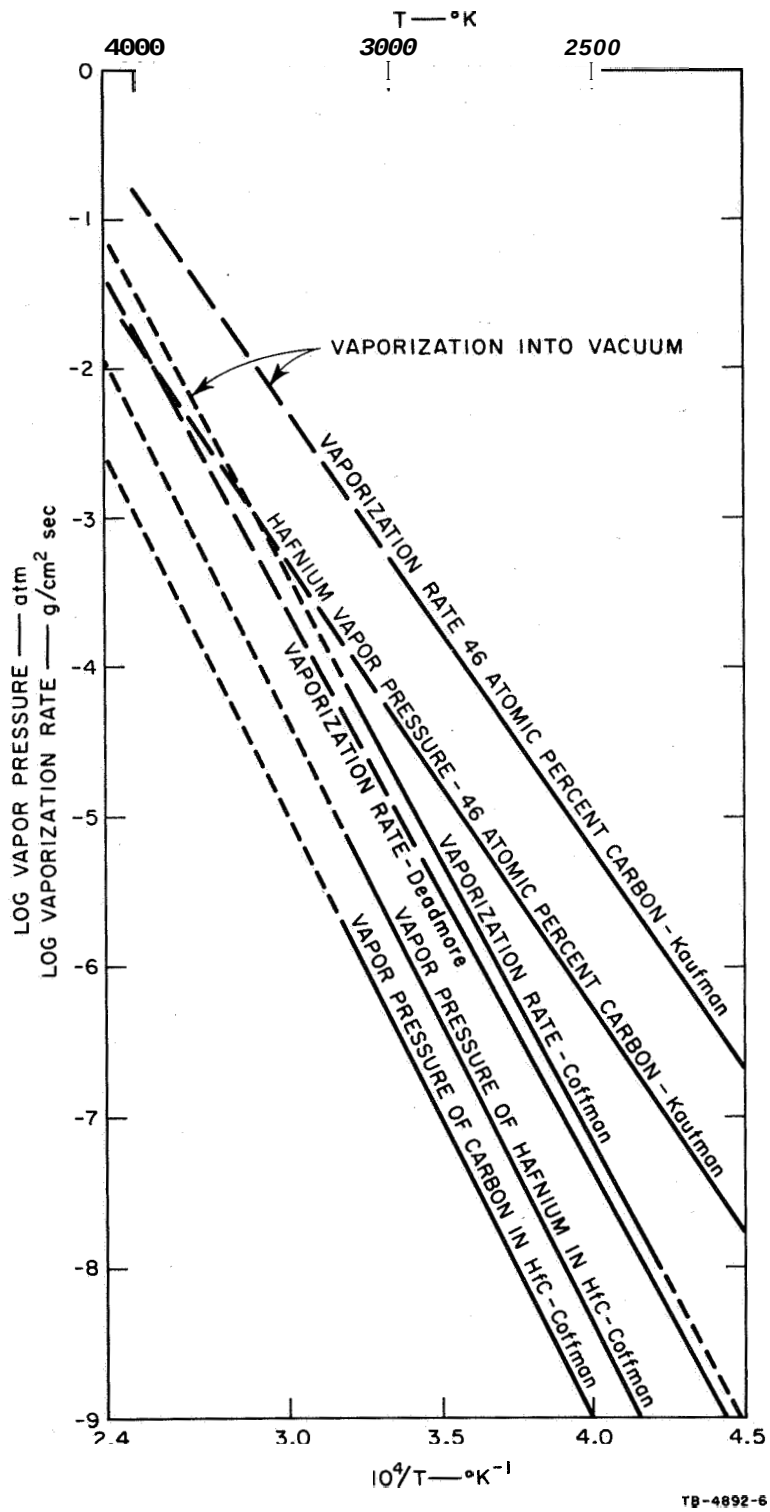

FIG. 31 VAPOR PRESSURE AND VAPORIZATION RATE FOR HAFNIUM CARBIDE

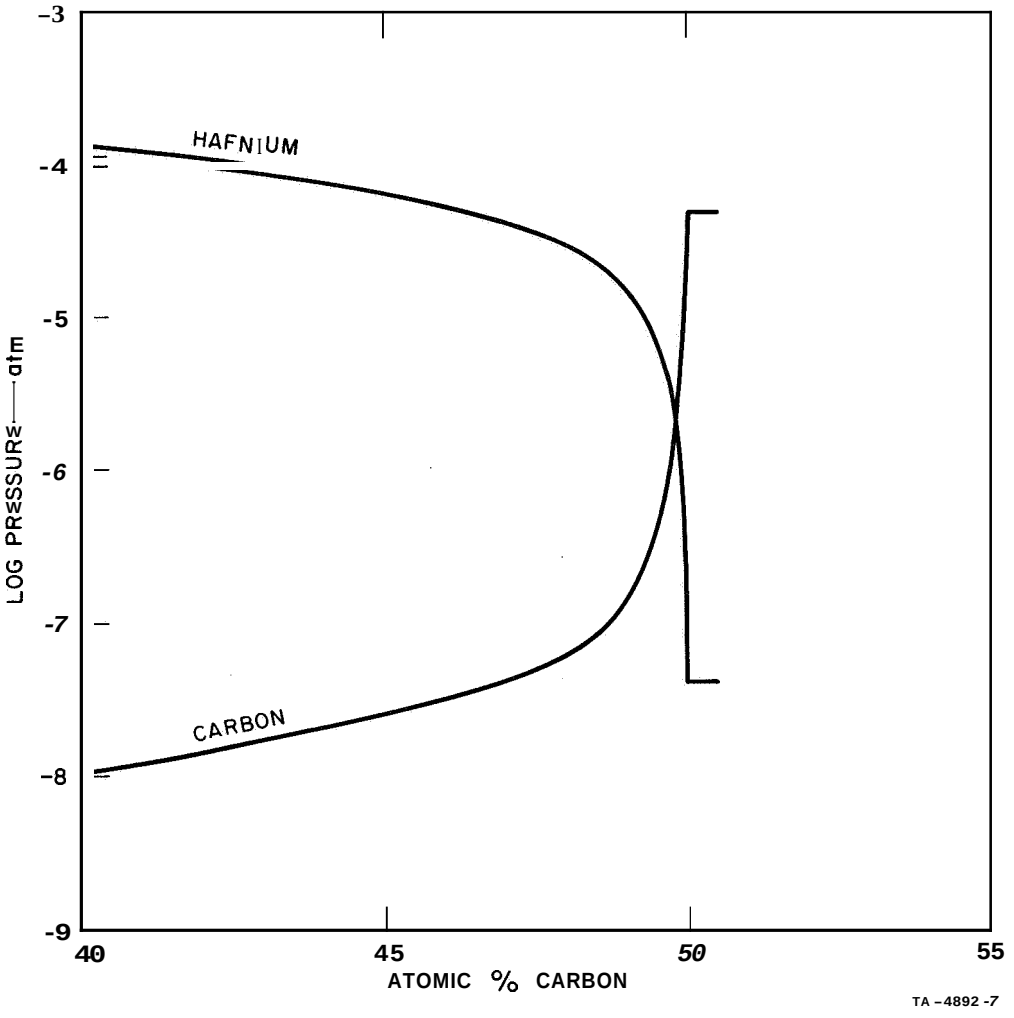

FIG. 32 CALCULATED VAPOR PRESSURES OF Hf AND C OVER HfC AT 3000°K **(Kaufman)**

APPENDIX B

THERMODYNAMIC AND KINETIC CONSIDERATIONS IN SOLUTION GROWTH OF TANTALUM CARBIDE

I. Thermodynamic Considerations

Free energy data are shown as a function of reciprocal temperature for a few carbides, including TaC, in Fig. 33. These data[27] are plotted as the log of the equilibrium constant, or the log of the product of the activities of the reactants in equilibrium with the carbide. As can be seen, tantalum carbide is a very stable compound and the tantalum activity and carbon activity in liquid metal solutions in equilibrium with tantalum carbide will be very low. The product of these activities at 1500°C is $(a_{Ta})(a_C) = 3.5 \times 10^{-5}$.

Consider the following cases.

Case 1. If crystal growth involves (1) a solvent metal, (2) tantalum added to the solvent, and (3) readily available carbon (e.g., graphite crucible), the system is not sufficiently specified in terms of the phase rule to be in equilibrium and a rapid irreversible reaction will proceed at elevated temperatures, precipitating tantalum carbide. If the graphite crucible is large enough, the reaction will continue until an insignificant amount of tantalum dissolved in the solution remains.

Under conditions of excess carbon at 1500°C, the tantalum acitivity will lower to 3.5×10^{-5}, since the carbon activity is fixed at $a_C = 1$ (see Fig. 33).

Case 2. If tantalum carbide is added to a liquid metal in a graphite crucible, it will dissolve until the tantalum activity, at 1500°C, reaches 3.5×10^{-5}. With the activity coefficients for tantalum that are expected in liquid transition metal's, the tantalum concentration will be below 0.01 at. %, too low to achieve appreciable tantalum transport and crystal growth in either Case 1 or 2.

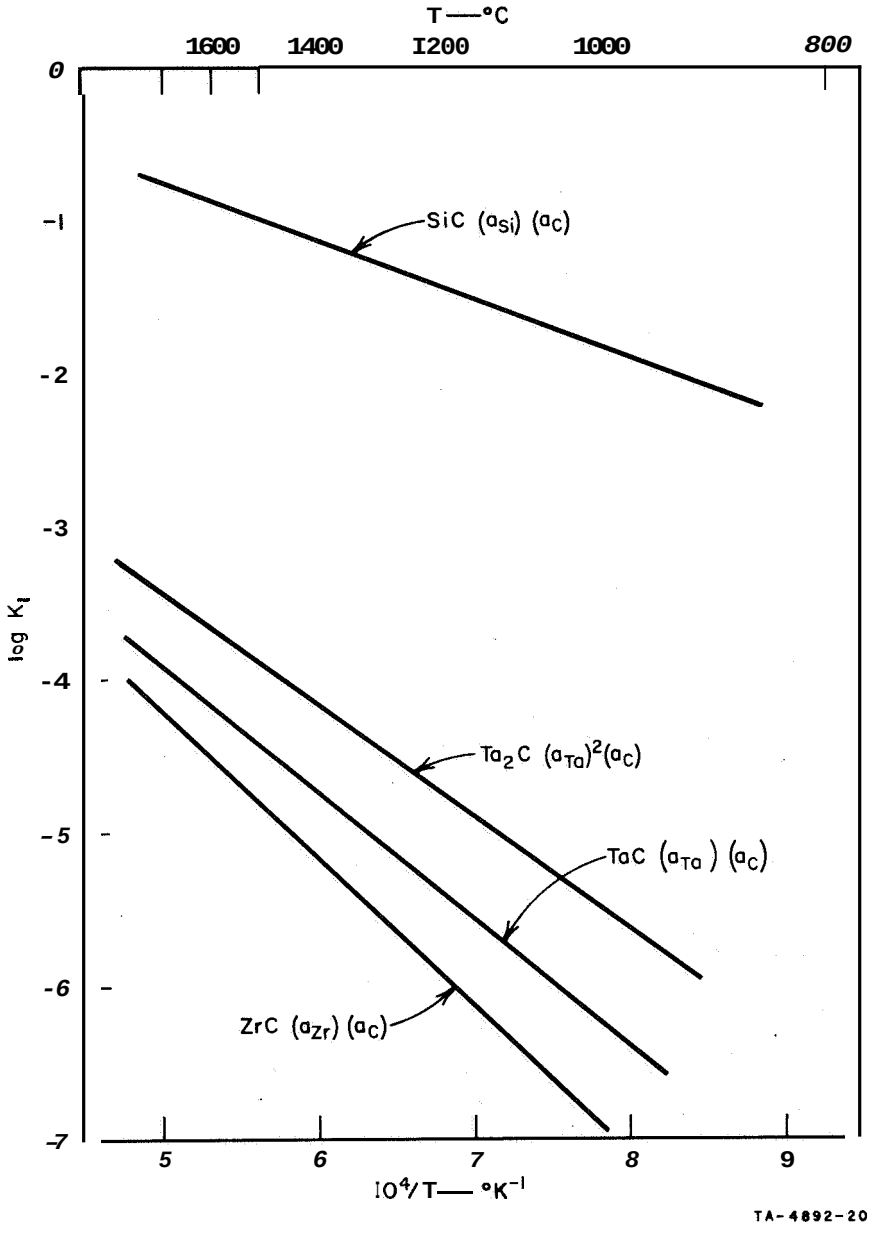

FIG. 33 FREE ENERGY OF FORMATION OF SEVERAL REFRACTORY CARBIDES, PLOTTED AS THE LOG OF THE REACTANT ACTIVITY PRODUCT VERSUS RECIPROCAL TEMPERATURE

Case 3. If tantalum carbide is used as the nutrient and an inert crucible is used in lieu of graphite, then the tantalum acticity will be raised considerably while the carbon activity is depressed correspondingly when compared with Cases 1 and 2. In the unlikely event that the activity coefficients for tantalum γ_{Ta} and carbon γ_C are equal, then the activities of tantalum and carbon will both be equal to $K_1^{1/2}$, or 5.9×10^{-3} at 1500°C. Thus, using an inert crucible and a tantalum carbide nutrient should be more favorable to the mass transport of tantalum, without unduly supressing the mass transport of carbon, and this will favor more rapid crystal growth.

Tantalum and carbon activities during growth of tantalum carbide at 1500°C under the three cases are shown in Table XII. The purpose of this table is to indicate the wide variation in activities that will occur, depending on whether separate tantalum and carbon sources are present or whether tantalum carbide is the only source of both solutes.

Table XII

TANTALUM AND CARBON ACTIVITIES DURING GROWTH OF TANTALUM CARBIDE AT 1500°C

Melt System	Carbo: Activity		Tantalum Activity		Growth Condition
	Initial	Equilibrium	Initial	Equilibrium	
Excess tantalum and carbon crucible (Case 1)	1	1	$1 \geq a_{Ta} >> 3.5\times10^{-5}$*	3.5×10^{-5}	Irreversible
TaC nutrient and carbon crucible (Case 2)		1	3.5×10^{-5}	3.5×10^{-5}	Reversible (thermal gradient)
TaC nutrient and inert crucible (Case 3)	5.9×10^{-3}†	5.9×10^{-3}†	5.9×10^{-3}†	5.9×10^{-3}†	Reversible (thermal gradient)

* If enough tantalum metal is added to the melt to saturate it, then $a_{Ta} = 1$. The tantalum activity will be reduced for smaller additions.

† Provided that $\gamma_{Ta} = \gamma_C$.

Although activity coefficients are unknown for tantalum in any liquid metal, the mole fractions, X_i, of tantalum and carbon in solution are related to their activities:

$$a_i = \gamma_i X_i$$

Since the goal of this investigation was to grow large crystals, it appeared desirable to limit the supersaturation (excess concentration) of tantalum or carbon with respect to tantalum carbide in order to prevent excessive nucleation. If both excess tantalum and excess carbon are present in the melt system (irreversible case), a solvent with low solubility of one or both reactants is required to prevent excessive supersaturation. Conversely, if a tantalum carbide nutrient is used without a tantalum source (reversible case), a solvent with a high tantalum solubility (low activity coefficient) is required to increase the tantalum concentration to a high enough level to secure adequate mass transport rates in the solution.

Some additional considerations for the growth of tantalum carbide crystals irreversibly from dilute solutions and reversibly using a tantalum carbide nutrient are contained in the following sections.

11. Low Solubility Solvents for Irreversible Growth of Tantalum Carbide

Because the entropy of the solution is greater than that of the segregated solid phases, higher temperatures usually favor higher solubilities. Therefore an increase in temperature causes a decrease in chemical potential of the solute, which can only be offset by increased solution of the solute component. Since, for the irreversible case, moderately low solubilities are being sought, an examination of tantalum and carbon solubilities near the melting points of several liquid metals provides a guide to useful solvent systems.[28-30] Tantalum solubility data are presented in Table XIII, and carbon solubility data are shown in Table XIV.

Table XIII

TANTALUM SOLUBILITIES NEAR MELTING POINTS OF LIQUID METALS[28-30]

Solvent	Temperature (°C)	Tantalum Solubility (Wt %)	Tantalum Source
Aluminum	2680	0.15	$TaAl_3$
Iron	1534	>20	$TaFe_2$
Nickel	1453	>40	$TaNi_3$
Silicon	1405	> 6	$TaSi_2$
Tin		Unknown low	

Table XIV

CARBON SOLUBILITIES IN LIQUID METALS[28-30]

Solvent	Carbon Solubility (Wt %)	Eutectic Temperature (°C)
Chromium	3.0	1498
Cobalt	2.9	1300
Copper	<.001 (1400°C)	--
Iron	4.26	1153
Molybdenum	-3.5	2200
Nickel	2.1	1318
Silicon	3-4 (2300°C) 2.5×10^{-3} (1413°C)	1413
Aluminum	Unknown low	--
Tin	Unknown low	--

It appears that the transition metals are either too refractory or have high solubilities for tantalum and carbon. Lower solubilities are expected in metals from groups IB, IIB, IIIA, IVA, and VA. In most cases the solubility will probably be too low. This condition was observed with tin. The effective solvent properties obtained with a binary melt containing a solvent inactive metal, e.g., tin, and a solvent active metal, e.g., iron, are too complex for analysis or even speculation without experimental data. We have observed experimentally that the 10% iron and 90% tin alloy is an active solvent for carbon and tantalum.

III. Equilibrium Growth Using a Tantalum Carbide Nutrient and a Thermal Gradient

If TaC is the sole source for both tantalum and carbon in solution, then their concentrations must be equal in order to maintain a mass balance regardless of differences in their respective activity coefficients. The corollary to this is that their activities need not be equal. The activity product (a_C) (a_{Ta}), and not the individual activities, is governed by the TaC equilibrium constant K_1. Activity coefficients of carbon in several liquid metals have been determined, but no activity coefficient data for tantalum or hafnium were found during a literature search. The activity coefficient of zirconium[31] in liquid iron is $\gamma_{Zr} = 0.011$. The activity coefficient of carbon in liquid iron is $\gamma_C = 4$. If one ignores interactions in the ternary iron–carbon–tantalum system and predicts $\gamma_{Ta} = \gamma_{Zr}$, then concentrations of tantalum and carbon in liquid iron can be calculated. This was done and the results are graphed in Fig. 34. Calculated values based on use of an inert crucible are compared with values based on using a graphite crucible; $a_C = 1$. The upper and lower curves represent the carbon solubility and tantalum solubility, respectively, when a graphite crucible is employed. This is the equilibrium situation without free tantalum additions. Two values of the tantalum activity coefficient are used, $\gamma_{Ta} = 0.01$ and $\gamma_{Ta} = 1$. In both cases the tantalum solubility is below 1% at practical melt temperatures. Experience with SiC crystal growth[32] has shown that a solubility approaching 1% is desirable to obtain reasonable growth rates with the thermal gradient method.

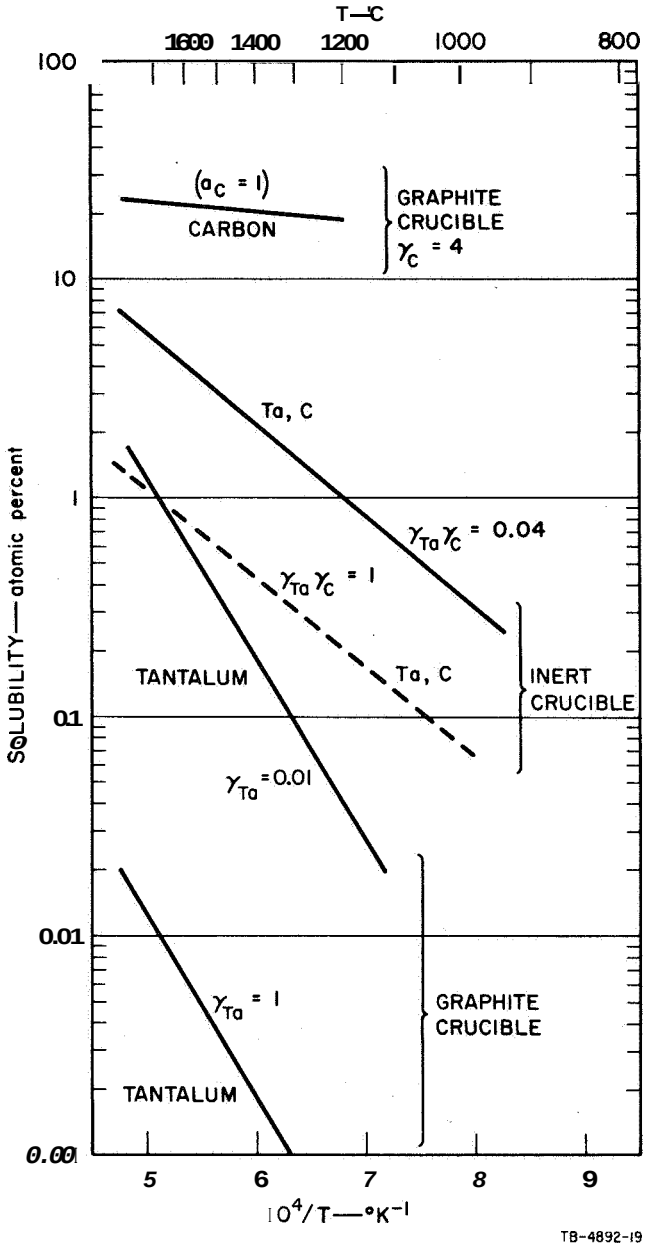

FIG. 34 CONCENTRATION OF TANTALUM AND CARBON IN EQUILIBRIUM WITH TaC IN AN IRON SOLVENT, WITH AND WITHOUT A CARBON CRUCIBLE; TANTALUM ACTIVITY COEFFICIENTS ARE ESTIMATED

For equilibrium dissolution and regrowth of TaC, stoichiometric considerations require the carbon and tantalum concentrations in the solution to be equal:

$$C_C = C_{Ta} \equiv C_i \qquad \text{(B-1)}$$

This requirement assumes that there are no chemical side reactions, in the melt or with the crucible or atmosphere, that remove either tantalum or carbon. Equation (B-1) and the equilibrium condition provide the following relation:

$$\gamma_{Ta}\ \gamma_C\ C_i^2 = K^{-1}$$

and

$$C_i = (K\ \gamma_{Ta}\ \gamma_C)^{-1/2} \qquad \text{(B-2)}$$

Activity coefficients usually vary slightly with temperature, but vary considerably with concentration.

IV. Kinetics of Crystal Growth

The rate of crystal growth can be no greater than the rate of transport of tantalum and carbon in the metal solution. If fluid mixing, caused by either thermal convection or mechanical stirring, is neglected, the transport rate J is given by Fick's first diffusion equation:

$$J = D\ \frac{dC}{dx} \qquad \text{(B-3)}$$

where D is the solute diffusion coefficient in the liquid metal solution, C is the solute concentration, and x is the diffusion distance, Under steady state crystal growth the diffusion equation is:

$$J = \frac{D\ (C_h - C_l)}{\delta_c} \qquad \text{(B-4)}$$

where C_h is the concentration at the higher temperature source, C_1 is the concentration in the liquid adjacent to the growing crystal, and δ_C is the distance between the source and the crystal. For the equilibrium growth of TaC in a chemically inert crucible, the source is usually TaC chips lying on the crucible bottom while the crystal is located near the melt meniscus. Thus, δ_C is equal to the liquid depth. When concentration C is expressed in atomic percent, the diffusion coefficient D in cm^2/sec and the transport rate J in cm/sec, for dilute solutions equation (B-4) is approximately

$$J\ (cm/sec) = \frac{D\ (C_h - C_1)}{100\ \delta_c} \left(\frac{M}{\rho}\right)_{soln} \left(\frac{\rho}{M}\right)_{TaC} \qquad (B-5)$$

Some reasonable estimates of most of the parameters in Equation (B-5) can be made. Diffusion coefficients in liquids at high temperatures are similar, $D \approx 10^{-4}\ cm^2/sec$. The diffusion distance is limited by free convection (without stirring) to $\delta \approx 1$ cm, even though actual melt depths are slightly greater than 1 cm. On this basis the TaC crystal growth rate dependence on the concentration difference from source to crystal can be estimated using Equation (B-5):

$$J \approx 10^{-6}\ (C_h - C_1)\ cm/sec$$
$$0.86\ (C_h - C_1)\ mm/day \qquad (B-6)$$

Forced stirring will increase the growth rate considerably, but this is not always convenient and there may be undesirable chemical reactions with the stirrer.

Plots of equilibrium concentration C_i versus the activity coefficient product $(\gamma_{Ta}\gamma_C)$ based on Equation (B-2) are shown for various temperatures in Fig. 35. In order to maximize the carbon and tantalum concentration and the crystal growth rate, a liquid metal solution that provides the lowest value of $(\gamma_{Ta}\gamma_C)$ must be sought. Superimposed on the concentration curves of Fig. 35 are two curves representing the values of $(\gamma_{Ta}\gamma_C)$ required to achieve the indicated crystal growth rates at

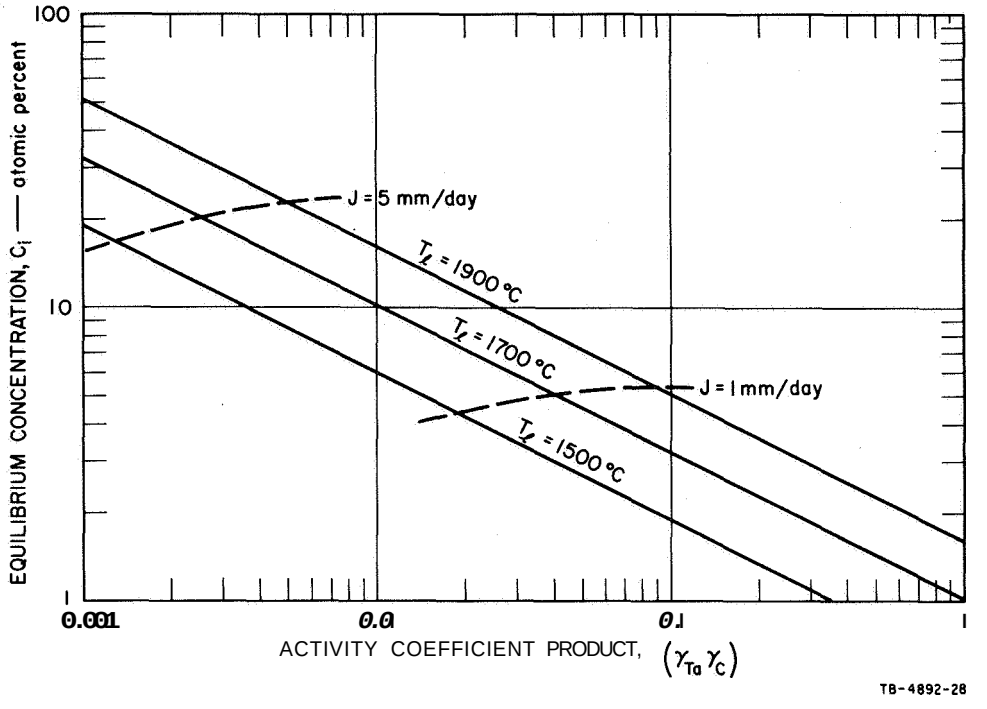

FIG. 35 EQUILIBRIUM CONCENTRATION OF Ta AND C AS A FUNCTION OF THEIR ACTIVITY COEFFICIENT PRODUCT

these temperatures. These curves are based on a 100°C temperature difference between source and crystal. Using an estimate of $\gamma_{Ta}^{Fe}\gamma_{C}^{Fe} \approx 0.06$, it would take a crystal growing temperature of 1800°C with a 1900°C source temperature to grow TaC at the rate of 1 mm/day (see Fig. 35).

It is expected that the lowest values of $\gamma_{Ta}\gamma_C$ will be found in those liquid metals that have a high solubility for both carbon and tantalum. This consideration and the need to avoid formation of other carbides point to the third period transition metals, vanadium through nickel. Although most of these metals form carbides, they can be used at least partially in alloys at crystal growing temperatures without carbide formation. The carbide forming tendency decreases when going from vanadium to nickel. With the exception of iron, little is known about the carbon activity in dilute solutions of carbon in these liquid metals. However, predictions as to whether the carbon activity coefficient is more or less than the carbon activity coefficient in liquid iron can be made from the

effect of these metals as alloying elements on the activity coefficient of carbon in liquid iron alloys. These data are shown in Fig. 36. Vanadium and chromium additives have the desirable effect of decreasing the activity coefficient of carbon. Managanese, not shown in Fig. 36, has a similar effect.[33]

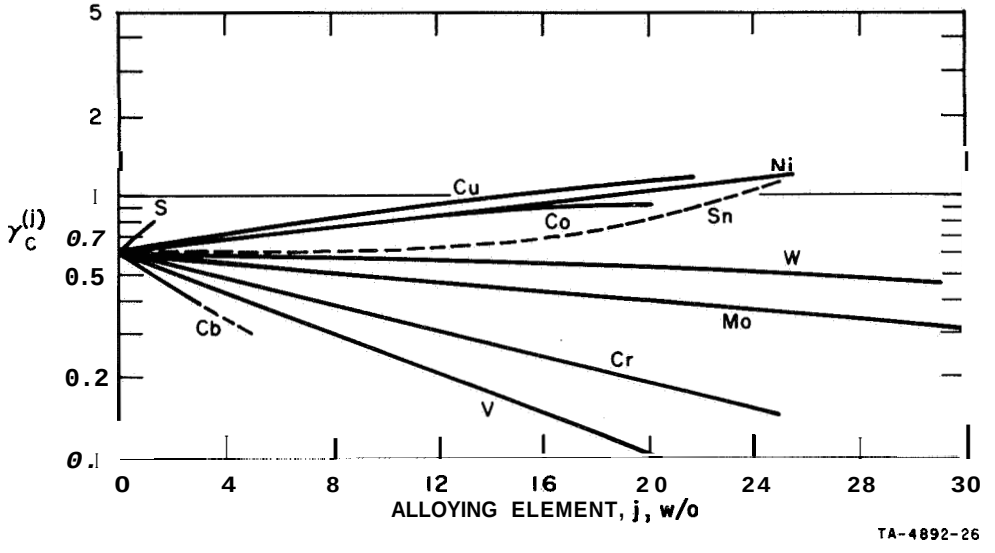

FIG. 36 EFFECT OF ALLOYING ELEMENTS ON ACTIVITY COEFFICIENT OF CARBON IN LIQUID IRON AT 1560°C FOR DILUTE SOLUTIONS OF CARBON IN IRON (after Elliott[31])

REFERENCES

1. Rudy, E., and D. P. Harmon, Ternary Phase Equilibria in Transition Metal–Boron–Carbon–Silicon Systems, Part I, Vol. V, AFML–TR–65–2, Dec. 1965.

2. Rudy, E., Ternary Phase Equilibria in Transition Metal–Boron–Carbon–Silicon Systems, Part I, Vol IV, AFML–TR–65–2, Sept. 1965.

3. Sanders, W. A., and S. J. Grisaffe, The Hot–Pressing of Hafnium Carbide, NASA TN D–303, 1960.

4. Sara, R. V., C. E. Lowell, and R. T. Dolloff, Research Study to Determine the Phase Equilibrium Relations of Selected Metal Carbides at High Temperatures, Tech. Doc. Rept. No. WADD TR 60–143, Part IV, Contr. No. AF 33(657)-8025, Feb. 1963.

5. Bowman, A. L., The Variation of Lattice Parameter with Carbon Content of Tantalum Carbide, J. Phys. Chem. 65, 1596 (1961).

6. Lesser, R. V., and G. Brauer, Karbidphasen des Tantals, Zeitschrift für Metallkunde 49, 622 (1958).

7. Deadmore, D. L., Vaporization of Tantalum Carbide-Hafnium Carbide Solid Solutions at 2500°K to 3000°K, NASA TMX–52014, 1964.

8. Deadmore, D. L., Influence of Time on Vacuum Vaporization Rate and Surface Compositional Stability of Tantalum Carbide–Hafnium Carbide Solid Solutions Above 2000°C, NASA TN D–3503, July 1966.

9. Santoro, G., and H. B. Probst, An Explanation of Microstructures in the Tantalum–Carbon System, Proceedings of the 12th Annual Conference on Applications of X–Ray Analysis, Aug. 7–9, 1963, Plenum Press, New York.

10. Johansen, H. A., and J. G. Cleary, The Ductile–Brittle Transition in Tantalum Carbide, J. Electrochem. Soc. 113, 378–81 (1966).

11. Reed, T. B., Induction–Coupled Plasma Torch, J. Appl. Phys. 32, 821 (1961).

12. Kittel, C., Introduction to Solid State Physics, John Wiley & Sons, New York, 1953, p. 90.

13. Hearmon, R. F. S., An Introduction to Applied Anisotropic Elasticity, Oxford University Press, New York, 1961, Chap. 6.

14. Gilman, J. J., and B. W. Roberts, Elastic Constants of TiC and TiB_2, J. Appl. Phys. 32, 1405 (1961).

15. Williams, W. S., Influence of Temperature, Strain Rate, Surface Condition and Composition on the Plasticity of Transition Metal Carbide Crystals, J. Appl. Phys. 35, 1329–38 (1964).

16. Hoch, M., P. E. Blackburn, D. P. Dingledy, and H. L. Johnston, The Heat of Sublimation of Carbon, J. Phys. Chem. 59, 97 (1955).

17. Coffman, J.A., G. M. Kibler, T. R. Riethof, and A. A. Watts, Carbonization of Plastics and Refractory Materials Research, WADD Technical Report 60-646, Part I, pp. 40-53, 1961.

18. Kaufman, L., personal communication with H. B. Probst, Lewis Research Laboratories, NASA.

19. Eberle, V. L., Verdampfungsverhalten Hochschmelzender Karbide für Thermionische Stromerzeuger, Die Atomwirtschaft 5, 220 (1964).

20. Kempter, C. P., and M. R. Nadler, Thermal Decomposition of Niobium and Tantalum Monocarbides, J. Chem. Phys. 32, 1477 (1960).

21. Fries, R. J., Vaporization Behavior of Niobium Carbide, J. Chem. Phys. 37, 320 (1962).

22. Jones, H. A., I. Langmuir, and G. M. J. Mackay, The Rates of Evaporation and the Vapor Pressures of W, Mo, Pt, Ni, Fe, Cu, and Ag, Phys. Rev. 30, 201 (1927).

23. Fonda, G. R., Evaporation Characteristics of Tungsten, Phys. Rev. 21, 343 (1923).

24. Fonda, G. R., Evaporation of Tungsten Under Various Pressures of Argon, Phys. Rev. 31, 260 (1928).

25. Perry, J. H., et al., Chemical Engineers Handbook, 4th Ed., McGraw-Hill, New York, 1961, pp. 14-21. Also: Wilke, C. R., and C. Y. Lee, Estimation of Diffusion Coefficients for Gases and Vapors, Ind. Eng. Chem. 47, 1253 (1955).

26. Coffman, J. A., G. M. Kibler, T. F. Lyon, and B. D. Acchione, Carbonization of Plastics and Refractory Materials Research, WADD Technical Report 60-646, Part 11, pp. 41-46, 85-91, 1963.

27. Elliott, J. F., and M. Gleiser, Thermochemistry for Steel Making, Vol. I, Addison-Wesley, Reading, Mass., 1960.

28. Hansen, M., Constitution of Binary Alloys, McGraw-Hill, New York, 1958.

29. Battelle Memorial Institute, Binary and Ternary Phase Diagrams of Columbium, Molybdenum, Tantalum, and Tungsten, DMIC Report 152, Columbus, Ohio, April 1961.

30. Battelle Memorial Institute, Binary and Ternary Phase Diagrams of Columbium, Molybdenum, Tantalum, and Tungsten, DMIC Report 183, Columbus, Ohio, February 1963.

31. Elliott, J. F., and M. Gleiser, Thermochemistry for Steel Making, Vol. 11, Addison-Wesley, Reading, Mass., 1963.

32. Halden, F. A., A. Rosengreen, and W. E. Nelson, "Growth and Characterization of β-Silicon Carbide Single Crystals," Air Force Cambridge Research Laboratories, Report 65-206, Stanford Research Institute, May 1965.

33. Skiredj, O., and J. F. Elliott, Carbon Content of Graphite-Saturated Fe-Si-Mn Alloys, 1400 to 1650°C, Trans. AIME 227, 526 (1963).

STANFORD RESEARCH INSTITUTE

333 Ravenswood Avenue
Menlo Park, California 94025

Tel. (415) 326-6200
Cable: STANRES, MENLO PARK
TWX: 910-373-1246

Regional Offices and Laboratories

Southern California Laboratories
820 Mission Street
South Pasadena, California 91030
Tel. (213) 799-9501 • 682-3901

SRI-Washington
1000 Connecticut Avenue, N.W.
Washington, D.C. 20036
Tel. (202) 223-2660
Cable: STANRES, WASH.D.C.
TWX: 710-822-9310

SRI-New York
270 Park Avenue, Room 1770
New York, New York 10017
Tel. (212) 986-6494

SRI-Huntsville
Missile Defense Analysis Office
4810 Bradford Blvd., N.W.
Huntsville, Alabama 35805
Tel. (205) 837-3050
TWX: 510-579-2112

SRI-Detroit
303 W. Northland Towers
15565 Northland Drive
Southfield (Detroit), Michigan 48075
Tel. (313) 444-1185

SRI-Chicago
10 South Riverside Plaza
Chicago, Illinois 60606
Tel. (312) 236-6750

SRI-Europe
Pelikanstrasse 37
8001 Zurich, Switzerland
Tel. 27 73 27 (Day/Night) • 27 81 21 (Day)
Cable: STANRES, ZURICH

SRI-Scandinavia
Skeppargatan 26
Stockholm O, Sweden
Tel. 60 02 26; 60 03 96; 60 04 75

SRI-Japan
Nomura Securities Building
1-1 Nihonbashidori, Chuo-ku
Tokyo, Japan
Tel. Tokyo 271-7108
Cable: STANRESEARCH, TOKYO

Representatives

Canada
Cyril A. Ing
86 Overlea Boulevard
Toronto 17, Ontario, Canada
Tel. (416) 425-5550

Italy
Lorenzo Franceschini
Via Macedonio Melloni 49
Milan, Italy
Tel. 72 3246